

**ISTANBUL TECHNICAL UNIVERSITY ★ GRADUATE SCHOOL OF SCIENCE**  
**ENGINEERING AND TECHNOLOGY**

**FORMATION AND INVESTIGATION OF  
ORGANIC-INORGANIC COMPOUND STRUCTURES ON THE SURFACES  
AT NANOSCALE WITH SCANNING PROBES**

**M.Sc. THESIS**

**Elif PEKSU**

**Department of Physics Engineering**

**Physics Engineering Programme**

**JANUARY 2013**



**ISTANBUL TECHNICAL UNIVERSITY ★ GRADUATE SCHOOL OF SCIENCE**  
**ENGINEERING AND TECHNOLOGY**

**FORMATION AND INVESTIGATION OF  
ORGANIC-INORGANIC COMPOUND STRUCTURES ON THE SURFACES  
AT NANOSCALE WITH SCANNING PROBES**

**M.Sc. THESIS**

**Elif PEKSU  
(509081105)**

**Department of Physics Engineering**

**Physics Engineering Programme**

**Thesis Advisor: Assoc. Prof. Dr. Oğuzhan GÜRLÜ**

**JANUARY 2013**



**İSTANBUL TEKNİK ÜNİVERSİTESİ ★ FEN BİLİMLERİ ENSTİTÜSÜ**

**NANO ÖLÇEKTE TARAMALI UÇ İLE ORGANİK VE İNORGANİK  
BİLEŞİKLERİN ÇEŞİTLİ YÜZEYLERDE OLUŞUMU VE ARAŞTIRILMASI**

**YÜKSEK LİSANS TEZİ**

**Elif PEKSU  
(509081105)**

**Fizik Mühendisliği Anabilim Dalı**

**Fizik Mühendisliği Programı**

**Tez Danışmanı: Doç. Dr. Oğuzhan GÜRLÜ**

**OCAK 2013**



**Elif PEKSU**, a **M.Sc.** student of ITU **Graduate School of Science Engineering and Technology** student ID **509081105**, successfully defended the **thesis** entitled **FORMATION AND INVESTIGATION OF ORGANIC-INORGANIC COMPOUND STRUCTURES ON THE SURFACES AT NANOSCALE WITH SCANNING PROBES**", which she prepared after fulfilling the requirements specified in the associated legislations, before the jury whose signatures are below.

**Thesis Advisor :**      **Assoc. Prof. Dr. Oğuzhan GÜRLÜ**      .....  
İstanbul Technical University

**Jury Members :**      **Prof. Dr. Gönül ÖZEN**      .....  
İstanbul Technical University

**Asst. Prof. Dr. Nuri SOLAK**      .....  
İstanbul Technical University

**Date of Submission : 17 DECEMBER 2012**  
**Date of Defense :      24 JANUARY    2013**





*To my family,*



## **FOREWORD**

In this work, I would like to appreciate of my valuable supervisor Assoc. Prof. Dr. Oğuzhan GÜRLÜfor giving very useful information and guideness, which is particularly helpful at every stage of the study. I would like to thank Prof. Dr. FatmaTepahan from Physics Engineering Department, ITU for giving the opportunity to study with atomic force microscopy. I am thankful to Assoc. Prof. Dr. Alkan Kabakçioğlu from Physics Department, Koç University for giving the DNA molecules. I would like to thank Prof. Dr. Erol Okan from Physics Department, Trakya University. I am very thankful to all NANOBEES's members for their helps and special thanks to my family for their great and unlimited support.

DECEMBER 2012

Elif PEKSU  
(Physicist)



## TABLE OF CONTENTS

|  | <u>Page</u>  |
|--|--------------|
| <b>FOREWORD</b> .....  | <b>ix</b>    |
| <b>TABLE OF CONTENTS</b> .....                                 | <b>xi</b>    |
| <b>LIST OF TABLES</b> .....                                    | <b>xv</b>    |
| <b>LIST OF FIGURES</b> .....                                   | <b>xvii</b>  |
| <b>SUMMARY</b> .....   | <b>xxi</b>   |
| <b>ÖZET</b> .....  | <b>xxiii</b> |
| <b>1. INTRODUCTION</b> .....                                   | <b>1</b>     |
| 1.1 Purpose of Thesis .....                                    | 2            |
| <b>2. METHODS</b> .....  | <b>5</b>     |
| 2.1 Sample Preparation Techniques .....                        | 5            |
| 2.1.1 Drop casting method .....                                | 5            |
| 2.1.2 Drying in desiccator .....                               | 5            |
| 2.1.3 Annealing .....  | 6            |
| 2.2 Imaging Analysis .....                                     | 6            |
| 2.2.1 Optical microscopy .....                                 | 6            |
| 2.2.2 Scanning tunneling microscopy .....                      | 6            |
| 2.2.3 Atomic force microscopy .....                            | 8            |
| 2.2.4 Contact mode .....                                       | 12           |
| 2.2.5 Non-Contact mode .....                                   | 13           |
| 2.2.6 Intermittent (tapping or dynamic) mode .....             | 13           |
| 2.2.7 Phase imaging .....                                      | 14           |
| 2.2.8 Electrostatic force microscopy .....                     | 14           |
| 2.2.9 Raman microscopy .....                                   | 16           |
| 2.3 Substrates .....   | 18           |
| 2.3.1 Highly oriented pyrolytic graphite (HOPG) .....          | 18           |
| 2.3.2 Mica .....   | 19           |
| 2.3.3 Gold on Mica (Au 111) .....                              | 20           |
| 2.4 Solvent .....  | 21           |
| 2.4.1 DI water .....   | 21           |
| 2.4.2 Toluene .....  | 21           |
| <b>3. INVESTIGATION OF SOLVENT EFFECT</b> .....                | <b>23</b>    |
| 3.1 Experiments .....  | 23           |
| 3.1.1 Water effect on HOPG and mica .....                      | 23           |
| 3.1.2 Toluene effect .....                                     | 27           |
| <b>4. INVESTIGATION OF CdSe AND InP/ZnS QUANTUM DOTS</b> ..... | <b>29</b>    |
| 4.1 Quantum Dots .....   | 29           |
| 4.1.1 The excitation bohr radius .....                         | 30           |
| 4.1.2 Quantum confinement .....                                | 30           |
| 4.2 Experiments .....  | 32           |
| <b>5. INVESTIGATION OF DNA</b> .....                           | <b>51</b>    |

|                              |           |
|------------------------------|-----------|
| 5.1 Literature Review .....  | 51        |
| 5.2 Experiments .....        | 52        |
| <b>6. CONCLUSIONS.....</b>   | <b>61</b> |
| <b>REFERENCES.....</b>       | <b>63</b> |
| <b>APPENDIX .....</b>        | <b>69</b> |
| <b>CURRICULUM VITAE.....</b> | <b>73</b> |

## **ABBREVIATIONS**

|             |                                     |
|-------------|-------------------------------------|
| <b>AFM</b>  | : Atomic Force Microscope           |
| <b>DNA</b>  | : Deoxyribonucleic Acid             |
| <b>DOS</b>  | : Density of States                 |
| <b>EFM</b>  | : Electrostatic Force Microscope    |
| <b>HOPG</b> | : HighlyOriented Pyrolytic Graphite |
| <b>QD</b>   | : Quantum Dot                       |
| <b>SPM</b>  | : Scanning Probe Microscopy         |
| <b>STM</b>  | : Scanning Tunneling Microscopy     |





## LIST OF TABLES

|   | <b><u>Page</u></b> |
|---|--------------------|
| <b>Table 4.1</b> : Nanostructures , Their Confinements and DOS.....         | 31                 |
| <b>Table 4.2</b> : Properties of CdSe quantum dots 640nm Sigma Aldrich..... | 32                 |
| <b>Table 4.3</b> : Samples and results-1.....                               | 47                 |
| <b>Table 4.4</b> : Samples and results-2.....                               | 48                 |
| <b>Table 4.5</b> : Samples and results-3.....                               | 48                 |
| <b>Table 4.6</b> : Samples and results-4.....                               | 49                 |
| <b>Table 4.7</b> : Samples and results-5.....                               | 49                 |



## LIST OF FIGURES

|  | <u>Page</u> |
|--|-------------|
| <b>Figure 1.1</b> : Quantum Dots.....  | 3           |
| <b>Figure 1.2</b> : DNA Structures .....   | 3           |
| <b>Figure 2.1</b> : Desiccators.....   | 5           |
| <b>Figure 2.2</b> : Optical Microscope. ....   | 6           |
| <b>Figure 2.3</b> : Scanning Tunneling Microscope.....   | 7           |
| <b>Figure 2.4</b> : TheSTM Principle. ....   | 8           |
| <b>Figure 2.5</b> : Atomic Force Microscope. ....  | 9           |
| <b>Figure 2.6</b> : Principle of atomic force microscopy.....  | 9           |
| <b>Figure 2.7</b> : Beam deflection system,using a laser and photodiode to measure the<br>beam position. ....  | 10          |
| <b>Figure 2.8</b> : AFM cantilever.....  | 11          |
| <b>Figure 2.9</b> : Interatomic force versus distance curve. ....  | 12          |
| <b>Figure 2.10</b> : Phase imaging.....  | 14          |
| <b>Figure 2.11</b> : Principle of Electrostatic Force Microscope. ....   | 15          |
| <b>Figure 2.12</b> : Capacitor.....  | 16          |
| <b>Figure 2.13</b> : Energy diagram for Rayleigh and Raman Scattering.....   | 17          |
| <b>Figure 2.14</b> : Raman spectroscopy system.....  | 18          |
| <b>Figure 2.15</b> : The Structure of The Bulk Hexagonal Graphite Crystal. ....  | 19          |
| <b>Figure 2.16</b> : Mica sheets. ....   | 20          |
| <b>Figure 2.17</b> : Gold on mica .....  | 20          |
| <b>Figure 3.1</b> : Hydrophobic and Hydrophilic Surfaces.....  | 23          |
| <b>Figure 3.2</b> : (a) HOPG-13 and (b) Mica Surface.....  | 24          |
| <b>Figure 3.3</b> : (a), (b); Optical Microscope Images, (c) AFM - Merck Water on HOPG-<br>13,(d) AFM - Merck Water on Mica.....   | 24          |
| <b>Figure 3.4</b> : Sample-357, 2 $\mu$ l VWR Water Drop Casted on HOPG-13, (a) Optical<br>Microscope Image, (b) and (c) AFM Images of Sample-357 .....  | 25          |
| <b>Figure 3.5</b> : Sample-373, 1 $\mu$ L VWR water was drop casted on HOPG-13(a) is<br>HOPG-13 with sample holder, (b) is optical image of Sample-373 after<br>drop castedon water, (c) is optical image of Sample-373 a day later<br>and(d) is AFM image of Sample-373 ..... | 26          |
| <b>Figure 3.6</b> : (a) Clean HOPG-13 and (b) Sample-468, water drop cased on HOPG-13<br>using our water system, ELGA.....   | 26          |
| <b>Figure 3.7</b> : Sample-401, 1 $\mu$ l toluene drop casted on HOPG-13.....  | 27          |
| <b>Figure 4.1</b> : Exciton Bohr Radius.....   | 30          |
| <b>Figure 4.2</b> : Structure of Quantum Dot.....  | 31          |
| <b>Figure 4.3</b> : Ligands of CdSe Quantum Dots. Ligand A; Hexadecylamine (HDA)<br>and B; Tri-Octylphosphine Oxide (TOPO).....  | 32          |
| <b>Figure 4.4</b> : (a), (b) AFM Images (c) Optic Microscope Image, (d) Height Profile of<br>the Sample-300.....   | 33          |

|   |    |
|---|----|
| <b>Figure 4.5:</b> (a), (b) AFM Images of Sample-300 in Different Area, (c) Height of Sample-300.....   | 34 |
| <b>Figure 4.6 :</b> Sample-338, (a) is Optical Image (b) is AFM Image, 1 $\mu$ l QDs Solution (Diluted by 2.5/5000 with Toluene) Drop Casted on HOPG-9 Surface.....   | 35 |
| <b>Figure 4.7 :</b> Sample-354, 1 $\mu$ l QDs Solution (Diluted by 2.5/7000 with Toluene) Drop Casted on Cleaved Mica Surface.....  | 35 |
| <b>Figure 4.8 :</b> Sample-375, Gold on Mica (Au 111).....  | 36 |
| <b>Figure 4.9 :</b> Sample-380, 1 $\mu$ l CdSe QD Solution (Diluted by 2.5/5000 with Toluene) Drop Casted on Flat Gold (Au 111) Surface (Sample-375). (a) Optical Microscope Image of Sample-380, (b) AFM Image of Sample-380.....  | 36 |
| <b>Figure 4.10:</b> Sample-392 (Gold Coated Mica), (b) Sample-398, 1 $\mu$ l CdSe QD Solution (non-diluted) Drop Casted on Sample-392.....  | 37 |
| <b>Figure 4.11:</b> Sample-393, 1 $\mu$ l QD Solution (Diluted by 2.5/5000 with Toluene) Drop Casted on HOPG-9, There are Stains on the Surface .....   | 37 |
| <b>Figure 4.12:</b> (a) Sample-411 and (b) height profile of Sample-411... ..   | 38 |
| <b>Figure 4.13:</b> Sample-408, 1 $\mu$ l CdSe QD Solution (Diluted by 2.5/5000 with Toluene) Drop Casted on Freshly Cleaved Mica. ....   | 39 |
| <b>Figure 4.14:</b> Sample-475, 1 $\mu$ l CdSe QD Solution (Diluted by 1/6000 with Toluene) Drop Casted on HOPG-.....   | 39 |
| <b>Figure 4.15:</b> Raman Spectra of the Clean HOPG-14 and sample-475.....  | 40 |
| <b>Figure 4.16:</b> Sample-484, 1 $\mu$ l CdSe QD Solution (Diluted by 1/6000 with Toluene) Drop Casted on HOPG-9.....  | 41 |
| <b>Figure 4.17:</b> Sample-423 (a) optical image, (b) topography and (c) height 1 $\mu$ l InP/ZnS QD Solution (Diluted by 2.5/5000 with Toluene) Drop Casted on Freshly Cleaved Mica.....   | 42 |
| <b>Figure 4.18:</b> (a) Sample-486, 150nm Gold Coated Mica (Au 111), (b) Sample 491, (c) and (d) are their height profiles. 1 $\mu$ l InP/ZnS QD Solution Drop Casted on Sample-486 (non-diluted).....  | 43 |
| <b>Figure 4.19:</b> Sample-507, (a) topography and (b) phase and (c) height profile.....  | 44 |
| <b>Figure 4.20:</b> Sample-507, (a) topography and (b) height profile in the different area.....  | 45 |
| <b>Figure 4.21:</b> Sample-522, (a) topography and (b) height profile. ....   | 45 |
| <b>Figure 4.22:</b> (a) Sample-523 (a) topography and (b) phase image. ....   | 46 |
| <b>Figure 5.1:</b> Expected DNA Structure.....  | 53 |
| <b>Figure 5.2:</b> 1 $\mu$ l DNA Solution Drop Casted on Mica Surface. ....   | 53 |
| <b>Figure 5.3:</b> AFM Images of DNA Solution Drop Casted on HOPG Surface. (a) Topography, (b) Phase Image.....   | 54 |
| <b>Figure 5.4:</b> Sample-351, 1 $\mu$ l DNA Solution ((a- $\delta$ ) unhybridized and Not Heated 8 Oligos) Diluted by 1/50 Drop Casted on Mica, It was Rinsed with Merck Water and Placed in Desiccator to Dry.....  | 54 |
| <b>Figure 5.5:</b> Sample-350 , 1 $\mu$ l DNA Solution ((a- $\delta$ ) Unhybridized and Not Heated Oligos) Diluted by 1/50 Drop Casted on Mica, It was Placed in Desiccator to Dry for a few minutes and rinsed with Merck Water .....  | 55 |
| <b>Figure 5.6:</b> Sample-490 1 $\mu$ l DNA Solution ((a- $\delta$ ) Unhybridized and Not Heated 8 Oligos) Diluted by 1/50 Drop Casted on Mica , It was Placed in Desiccator to Dry for a Few Minutes and Rinsed with Merck Water. (a) Topography, (b) Phase Image, (c) height profile..... | 55 |

|  |    |
|--|----|
| <b>Figure 5.7:</b> Sample-461, 1 $\mu$ l DNA Solution Drop Casted on Mica (non-Diluted).....   | 56 |
| <b>Figure 5.8:</b> Sample-462, 1 $\mu$ l DNA Solution Drop Casted on Mica (Diluted by 1/50).....   | 56 |
| <b>Figure 5.9:</b> Sample-501, 1 $\mu$ l DNA Solution Drop Casted on HOPG-13 (Diluted by 1/20 with Pure Water).....                        | 57 |
| <b>Figure 5.10:</b> Sample-501, 1 $\mu$ l DNA Solution Drop Casted on HOPG-13 (Diluted by 1/20 with Pure Water) in the Different Area..... | 58 |
| <b>Figure 5.11:</b> Sample-501, 1 $\mu$ l DNA Solution Drop Casted on HOPG-13.....   | 58 |



# **FORMATION AND INVESTIGATION OF ORGANIC-INORGANIC COMPOUND STRUCTURES ON THE SURFACES AT NANOSCALE WITH SCANNING PROBES**

## **SUMMARY**

A nanoparticle is a microscopic particle of an inorganic material (e.g. CdSe, InP/ZnS) or organic material (e.g. virus) with a diameter less than 100 nm. Nanoparticles are of great scientific interest as they are effectively a bridge between bulk materials and atomic or molecular structures. A bulk material should have constant physical properties regardless of its size, but at the nano-scale this is often not the case. Nanostructured semiconductors with small size have been the focus of recent scientific research because of their important nonlinear optical properties, luminescent properties, quantum size effects and other important physical and chemical properties. In the past decade, low- dimensional materials such as nanometersize inorganic dots, tubes have been discovered which exhibited a wide range of electronic and optical properties that depend sensitively on both size and shape, and are of both fundamental and technological interest.

Quantum Dots are very small semiconductor materials which contain tens to a few hundreds of atoms with sizes of a few nanometers. They exhibit quantum confinement (typically less than 10 nm in diameter). They are potentially ideal building blocks for nanoscale electronics and optoelectronics.

Deoxyribonucleic acid (DNA) is very important organic structures for living creatures. DNA supplies the information necessary for cells to reproduce. It is also responsible for determining how a person looks. DNA often contains codes for diseases that are genetic, passed from parent to child. DNA is also important for researchers who determine the role genes play in complex diseases. Thus, it is also important to understand its morphological structure for the future experiments.

The main purpose of this research is investigation of CdSe and InP/ZnS quantum dots (especially single QD) and deoxyribonucleic acid (DNA) with using atomic force microscopy (AFM), scanning probe microscopy, Raman spectroscopy and investigation of their morphological, electronic and optical properties. CdSe and InP/ZnS quantum dots surface systems were investigated on different surfaces such as highly oriented pyrolytic graphite, mica and Au(111). Single QD was investigated for QD electroluminescence.

In this research, the behavior of DNA and DNA patterns (networks) were searched on the HOPG and mica when a very short DNA was used and also effects of various solvents are investigated on HOPG and mica surfaces.





# **NANO ÖLÇEKTE TARAMALI UÇ İLE ORGANİK VE İNORGANİK BİLEŞİKLERİN ÇEŞİTLİ YÜZEYLERDE OLUŞUMU VE ARAŞTIRILMASI**

## **ÖZET**

Bir nanoparçacık, 100 nm'den daha küçük çapa sahip virus, DNA gibi organik, CdSe gibi inorganik çok ufak parçacıklardır. Nanoparçacıklar, atomik veya moleküler yapılar ve bulk arasında etkin bir şekilde köprü olduğundan bilimsel açıdan çok büyük öneme sahiptir. Bir kristal yapıda boyutu ne olursa olsun sabit fiziksel özelliklere sahip olmalıdır fakat nano-ölçekte bu durum genellikle böyle değildir. Küçük boyutlu yarıiletken nanoyapılar önemli doğrusal olmayan optik özellikleri, ışık saçma özellikleri, kuantum ölçek etkileri ve diğer fiziksel ve kimyasal özelliklerinden dolayı son bilimsel araştırmaların odak noktası olmuştur. Geçtiğimiz son on yılda, şekline ve boyutuna bağlı çok çeşitli elektronik ve optik özellikleri ortaya koyan nanometre boyutundaki inorganik noktalar, tüpler gibi düşük boyutlu malzemeler keşfedilmiştir.

Elektronların serbest hareketinin tüm boyutlarda sınırlandırılması, kuantum nokta olarak adlandırılan sıfır boyutlu nano yapıların ortaya çıkmasına neden olmuştur. Kuantum Noktalar birkaç nanometre boyutlu ve içerisinde onlarca atomu barındıran çok küçük yarı iletken malzemelerdir. Kuantum noktalarının özellikleri en çok boyut ve içerdiği atomlara bağlıdır. Boyutlarının küçük olmasından dolayı kuantum noktalarının özellikleri üzerinde kolayca oynanabilir ve böylece bu parçacıklar yeni uygulamalarda kullanılabilir. Tüm boyutlarda güçlü sınırlandırma sonucu elde edilen kuantum nokta yapıları kesikli enerji seviyelerine ve kabuki yapılarına sahip olduklarından dolayı yapay atom olarak da adlandırılır. Böyle yapıların şekil ve boyutlarının deneysel olarak kontrol edilmesi sebebiyle potansiyel olarak, kuantum noktalar nanoboyutta elektronik ve optoelektronikler için ideal yapıtaşları haline gelmiştir. Tek elektron transistörler, kuantum bilgisayarları, kızılötesi fotodetektörler, hafıza elemanları gibi cihazlar kuantum noktaları kullanılarak geliştirilmeye başlanmıştır.

Deoksiribo nükleik asit (DNA) yaşayan varlıklar için çok önemli yapılardır. DNA hücreleri çoğaltmak için gerekli olan bilgiyi sağlar. Canlı sistem içerisinde metabolik faaliyetlerin başlatılması, yürütülmesi ve kontrolü DNA tarafından düzenlenir. Aynı zamanda kişinin nasıl görüldüğünden de sorumludur. DNA genellikle çocuğa anne ve babadan geçen genetik hastalıklar için kodlar içerir. Bunları inceleyen araştırmacılar için de çok önemlidir. Esasında bir çift zincirden oluşan DNA molekülünün kimyasal bileşimi temel ölçüde bilinmektedir. Canlı sisteminin hayatta kalması adına gerekli tüm kalıtsal bilgi bu zincirin diziliminde saklanmaktadır. Gerçekleşecek olan metabolik faaliyet hakkındaki bilginin saklandığı çiftli zincirin ilgili bölümünün, işlemin gerçekleşmesi adına açılıp stokastik olduğu düşünülen bir biçimde RNA ile eşleşerek bilgi aktarımı yaptığı bilinmektedir. Oldukça karmaşık bir biçimde gerçekleşen bu sistemin çalışma prensibini anlamak, genetik havuzda canlıların nasıl başkalaştığı gibi problemlerin yanı sıra hücresel faaliyetlerin

anlaşılmasına da ışık tutacaktır. Bu yüzden, gelecekteki uygulamaları için DNA'nın incelenmesi ve morfolojik yapısını anlamak önemlidir. Bu noktada zincirin fiziksel özellikleri üzerine çalışmalar önem kazanmaktadır.

Son yirmi senede gelişen deneysel teknikler, DNA'nın morfolojik ve elektronik yapısını incelemeyi olanaklı hale getirmiştir. Doksanlı yılların başlarında HOPG yüzeyi üzerinde DNA atomik kuvvet mikroskopisi ile görüntülenmiştir. Yine doksanlı yıllarda taramalı tünelleme mikroskobu ile DNA'nın iletkenliği ölçülmüştür. Farklı ortamlar içerisinde ve yüzeyler üzerinde, farklı boyutlarda ve dizilimlerdeki DNA sarmalları incelenmeye devam edilmektedir.

Bu araştırmanın asıl amacı, CdSe ve InP/ZnS kuantum noktalarının (özellikle tek kuantum noktanın) ve deoksiribo nükleik asidin (DNA) atomik kuvvet mikroskobu ve elektostatik kuvvet mikroskobu, optik mikroskop, taramalı tünelleme mikroskobu ve raman spektroskopisi kullanılarak araştırılması, onların morfolojik, elektronik ve optik özelliklerinin incelenmesidir.

Taramalı uç mikroskobisinde en dikkat çeken özellik atomik ve moleküler seviyede görüntü alabilmektir. Atomları tek tek görebilmek, onlarla oynayabilmek birçok alanda yeni keşifler demektir. Atomik kuvvet mikroskobu bugüne kadar yüzey özelliklerinin ve malzeme topografisinin incelenmesinde vazgeçilmez olmuştur. Taramalı tünelleme mikroskobu iletken, yarıiletken yüzeylerle iğne arasındaki tünelleme akımını ölçerken atomik kuvvet mikroskobu iğne ile yüzey arasındaki etkileşim kuvvetini ölçer. Burada yüzeyin taramalı tünelleme mikroskobunda olduğu gibi iletken olması gerekmiyor. Atomik kuvvet mikroskobu her çeşit yüzey için ve her çeşit ortamda kullanılabilir. Zaten burada da en çok kullanılan mikroskoptur. Taramalı tünelleme mikroskobunda daha küçük alanlar taranabilir, atomik çözünürlük elde edilebilir. Atomik kuvvet mikroskobunda bunu elde etmek zor. Bunu elde etmeye çalışırken yüzeye, örneğe zarar verme olasılığı yüksektir. Optik mikroskop ise özellikle örnek hazırladıktan sonra solüsyonun nereye nasıl dağıldığını göstermek için idealdir.

Yapılan çalışmada özellikle DNA'nın seçilen yüzey üzerinde nasıl bir morfolojide durduğunu gözlemek amacı ile atomik kuvvet mikroskobu ile çalışılmıştır. Farklı yüzeyler üzerinde farklı boylarda hazırlanmış DNA ların konulması ile hangi parametreler ile DNA zincirlerinin ne şekilde katlandığı ve dış koşullara nasıl tepki verdiği bu yöntemle araştırılmıştır. DNA içeren çeşitli çözeltiler aynı anda hem HOPG üzerine hem de mika üzerine damlatılıp kurutulduktan sonra atomik kuvvet mikroskobu ile gözlemlendi. Sadece damlatma ile de kalmayıp kuruduktan sonra örneği yıkama ve kurumadan örneği yıkama gibi farklı örnek hazırlama teknikleri kullanıldı. DNA' nın düz yüzeylerde küresel olmaya yönelmesi problemi ile birlikte DNA' nın içinde bulunduğu çözeltilerin de yüzeylerde oluşturduğu yapılar DNA' nın özelliklerinin anlaşılması için önem arz etmektedir. DNA zincirlerinin solüsyonlardan yüzeylere kaplanmalarının yanı sıra hibridize edilmiş ve belirli geometrik özellikleri ihtiva eden DNA yapılarının morfolojik özellikleri de incelendi.

Kuantum noktalar sadece çekirdekten oluşan ya da çekirdek ve çekirdeği saran kabuktan oluşan iki çeşit yapıya sahiptir. Çekirdek haldeki kuantum noktalar görünür bölgede ışık emisyonuna sahiptirler. InP gibi kızılötesi bölgede ışık emisyonu yapan kuantum noktalar da vardır. Çekirdek ve kabuktan oluşan kuantum noktalarda çekirdek, bant genişliği daha büyük olan yarıiletkenlerle kaplıdır. Çekirdeğin dışına eksiton sızmasını azaltır.

Şimdiye kadar gerekli sistemler kuruldu. Kuantum noktaları yüzeye yayma işlemleri gerçekleştirildi. HOPG, mika ve altın gibi farklı yüzeyler üzerinde CdSe gibi çekirdek haldeki ve InP/ZnS gibi çekirdek ve kabuktan oluşmuş kuantum noktalarının yüzey sistemleri araştırıldı. Elektroluminesans yapabilmek için tek kuantum nokta gözlemlenmeye çalışıldı.

Bu araştırmada, çok kısa DNA'lar kullanıldığında, DNA'nın HOPG ve mika üzerinde nasıl davrandığı incelendi. Hibridize DNA'lar gözlemlenmeye çalışıldı. Bunu yaparken kullanılan çözücülerin farklı yüzeylere farklı tepkiler verdiği keşfedildi ve bir de çeşitli çözücülerin farklı yüzeylerdeki etkileri de araştırıldı. Bu sayede elde ettiğimiz datanın gerçekte gözlemlemeye çalıştığımız malzeme mi yoksa örnek hazırlarken kullandığımız kimyasallardan mı kaynaklandığı anlaşılmış oldu. Bu da datanın doğruluğuna yardımcı olmakta. Çeşitli substratlar kullanıldı ve bunların farklı çözücülere tepkisi farklı oldu. HOPG yüzeyi hidrofobik bir yüzey, mika ise hidrofilik yani HOPG suyu sevmeyen, mika ise suyu seven yüzeyler. Örneğin mika yüzeyine su damlatıldığında hemen kuruyup giderken HOPG üstüne damlatıldığında durum farklı oldu. Bu da ölçümlere farklı şekillerde yansdı.

Bu çalışma aslında üç ana bölümden oluştu. İlkin kuantum noktaların incelenmesi oluştururken ikinci ve üçüncü kısım sırasıyla çözücülerin substratlara etkisi ve DNA zincirlerinin incelenmesi oluşturmıştır.



## 1. INTRODUCTION

In the last decade, quantum dots (QDs) have attracted attention of researchers on account of their wide applications in many fields of science. Their quantum confinement effects and tunable electronic and optical properties[1-3] make them ideal building blocks in nanosize. Quantum dots are defined as very small semiconducting nanocrystals consisted of group II-VI or III-V elements. They can be considered as zero dimensional and also as a particle of matter. Quantum dots are so small that addition or removal of an electron can change their properties in some useful way. Synthetic methods for preparation of QDs have been improved by optimizing reagents, ligands, solvents. Quantum dots (QDs) are semiconductor crystals with 2-10 nm (10-50 atoms) in diameter and they include up to a total of 100 to 100,000 atoms within the quantum dot volume[4-5]. The size of the crystal affects the band gap. The band gap is a very important factor determining the electrical conductivity of a semiconductor. In bulk, the bands are formed by the combination of neighboring energy levels of numerous atoms or molecules. Every particle is made up of only finite number of atoms in the smaller size and the number of overlapping energy levels decrease. Namely, the smaller size of the crystal cause the larger band gap. The larger the band gap, the greater the confinement on the movement of electrons. As the band gap is increased, we need more energy to excite the quantum dots and when the crystal returns to its ground state more energy releases.

Quantum dots were discovered in 1980s by Ekimov and Louis Brus in colloidal solutions and the term of quantum dot were coined by Mark Reed. Quantum dots have lots of features. They are applicable in many fields such as diode lasers, LEDs, solar cells etc. [6-7].

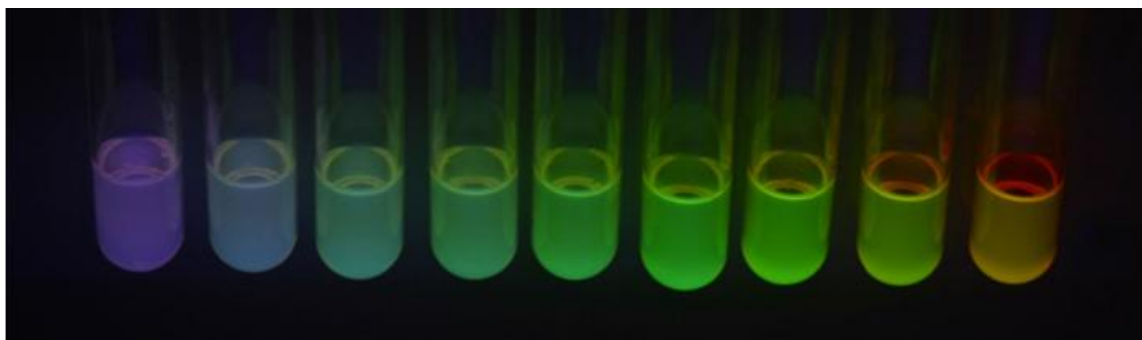
Deoxyribonucleic acid (DNA) is crucial structure for living creatures. DNA is an important biomacromolecule with remarkable chemical and biophysical properties [8-10]. Thus, it is also important to understand its morphological structure. The adsorption of single-stranded and double stranded DNA at the solid surface plays a

vital role in many fields and enables the chemical and structural modification of the sensor surface [11].

Atomic force microscopy (AFM) has proved to be a powerful tool for obtaining high-resolution images of DNA in air and in solution. Images of DNA conformations, unusual structures and DNA – protein complexes have been obtained almost exclusively on mica [12-15], but rarely on conducting materials. Effectively, the DNA molecules do not bind strongly enough to conducting substrates and the AFM tip tends to sweep away the adsorbed macromolecules. DNA has negative charge because of the phosphate ions and DNA is a highly charged, conductive and hydrophilic molecule.

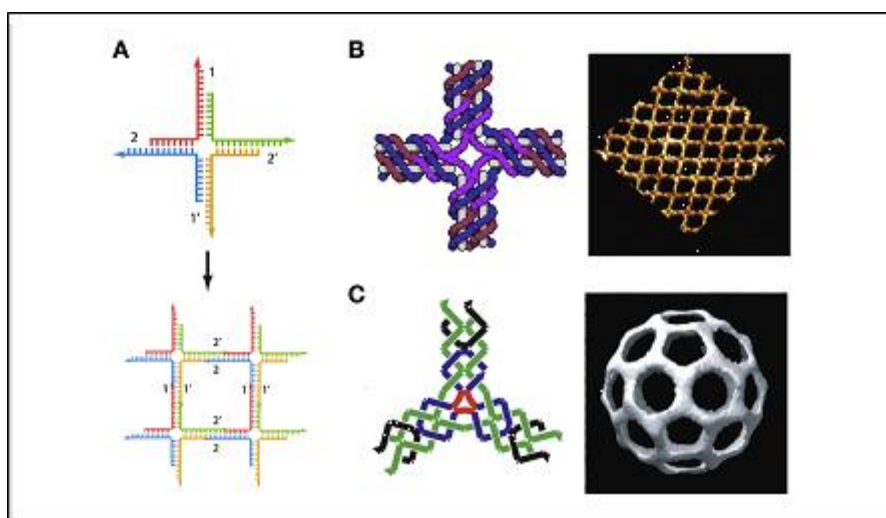
### **1.1 Purpose of Thesis**

The main purpose of this research, preparation of nano-structures and investigation of their morphological, electronic and optical properties using scanning probe techniques such as atomic force microscopy and electrostatic force microscopy and Raman spectroscopy. CdSe and InP/ZnS quantum dots were investigated on different surfaces such as highly oriented pyrolytic graphite (HOPG), mica and Au (111). In this study, firstly quantum dot solutions were prepared using different kinds of quantum dots such as core, core-shell quantum dots. Quantum dot solutions are shown in Figure 1.1. Quantum dots were homogeneously distributed on the different surfaces and it was checked using optic microscope. It was tried to observe single quantum dot in order to set up a substructure to make electroluminescence by use of the tunneling electrons from the tip of a scanning tunneling microscope. During experiments an optical microscope, an atomic force microscope (AFM), a scanning tunneling microscope (STM) and Raman spectroscopy was used.



**Figure 1.1 :** Quantum Dots [16].

DNA molecules tend to be spherical on the flat surfaces. If it stays plain, it becomes easy to measure conductivity. In this research, short and hybridized DNA segments were used. DNA structures are shown in Figure 1.2. The behaviors of DNA sequences were searched on the HOPG and mica when a short DNA was used and also effects of various solvents are investigated on HOPG and mica surfaces.



**Figure 1.2 :** DNA Structures [17].





## **2. METHODS**

### **2.1 Sample Preparation Techniques**

#### **2.1.1 Drop casting method**

Most used sample preparation technique is drop casting method. Before the drop casting, the surface should be clean enough. In this method, the required amount of solution is taken with a micropipette and dropped onto the surface. According to the features of the surface or solution, behaviour of the bubble changes. If the surface is hydrophobic when water is drop casted on it , it will stay intact on the surface as a ball.

#### **2.1.2 Drying in desiccator**

Desiccator is generally made of glass and after drop casting of the sample solution, the samples are placed in a desiccator to dry. It is used to preserve the sample from the moisture normally present in the atmosphere. Desiccator is a significant tool at sample preparation process. Desiccators are shown in Figure 2.1.



**Figure 2.1 : Desiccators.**

### **2.1.3 Annealing**

Annealing is a thermal process whereby a sample is heated to a particular temperature and then allowed to cool slowly[18]. It was used to remove the remnants from the surface. In this study annealing process was used in  $H_2$ -Ar atmosphere for quantum dots. Temperature is very important for this process otherwise we can damage the sample.

## **2.2 Imaging Analysis**

### **2.2.1 Optical microscopy**

Optical microscope is used for micron level investigations. Optical microscopy is the first step in order to investigate the samples before using scanning probe microscopes. Optical microscope images can tell us information about the surface and distribution of the solution. In this study Olympus BX51 Microscope was used. It is shown in Figure 2.2.

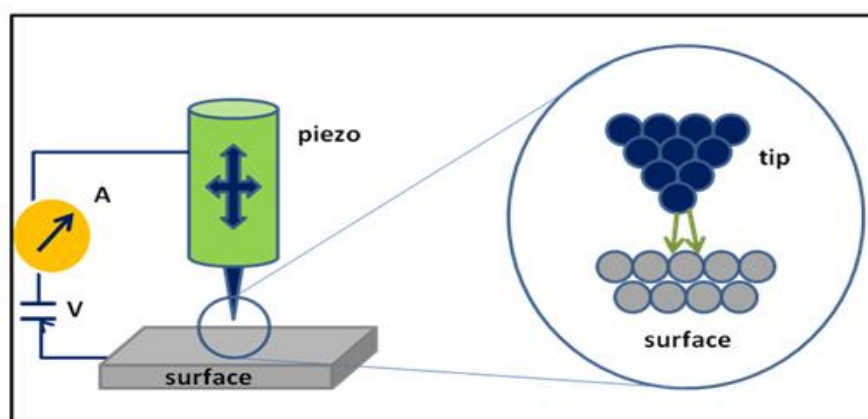


**Figure 2.2 : Optical Microscope.**

### **2.2.2 Scanning tunneling microscopy**

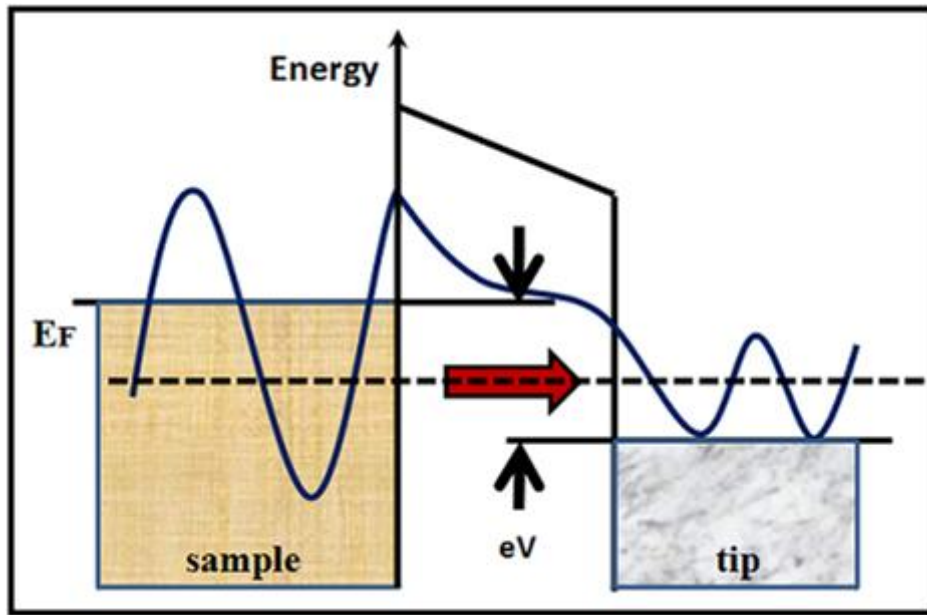
Scanning tunneling microscope was invented by Gerd Binnig and Heinrich Rohrer [19] which got them the Nobel prize for Physics in 1986 [20]. Scanning tunneling

microscope which is schematically shown in Figure 2.3 is a crucial device for surface characterization[19-21]. It can be used in air and vacuum. In the scanning tunneling microscope the sample is scanned by an atomically very sharp metallic tip [19]. STM tips are prepared by pull and cut method or electrochemically etching [20] using Pt/Ir or tungsten. The sample surface must be conducting or semiconducting [20] surface which is atomically flat and clean. The surface shall not be too rough.



**Figure 2.3 :** Scanning Tunneling Microscope.

There is very small distance between the tip and sample, approximately a few Å. This distance is controlled by the tunnel current flows when the tip is almost in contact with the sample[21]. The fine tip is mechanically connected to the scanner and the tip is moved in x,y,z directions via piezoelectric materials[23]. Piezoelectric materials expand or become smaller when a voltage is applied. The sample is negatively or positively biased so that a small current on the order of picoamperes flows between the sample and the tip. The feedback mechanism keeps the distance between tip and sample constant by means of the tunneling current[20-21]. If the tunnelling current increases, the distance between the tip and the sample is decreased, if the tunneling current decreases, the feedback mechanism increases the distance. The STM principle is shown in Figure 2.4. Nanosurf EasyScan2 STM was used during the all experiments.

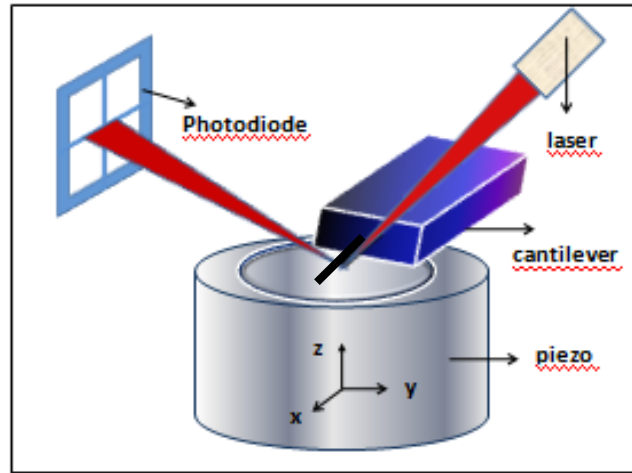


**Figure 2.4 : The STM Principle.**

### **2.2.3 Atomic force microscopy**

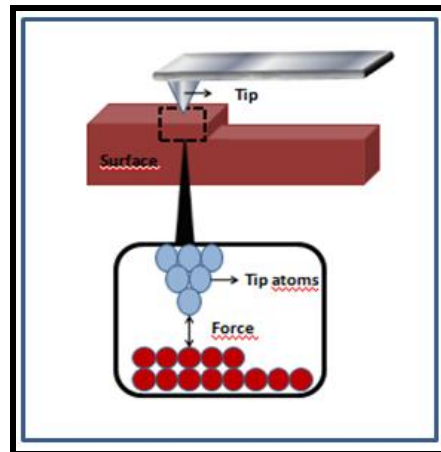
After invention of the Scanning tunnelling microscope (STM) Gerd Binnig, Calvin Quate and Christoph Gerber started researching a new type of microscope in order to investigate both insulators and conductors samples [21-22]. They invented atomic force microscope (AFM) to investigate the surfaces on an atomic scale in 1986. AFM looks like a blind person with a stick in order to explore the path [25]. In AFM, the sample is scanned with a cantilever. Deflection of the cantilever is recorded by a computer. AFM does not work according to tunnelling current like STM, it works according to forces between the tip and the surface [21-22, 24].

Atomic force microscope can work under several environments such as air, vacuum and liquid [26]. AFM is not like STM. It can be applied to various samples such as conductive or nonconductive surfaces, organic samples, soft biological samples etc. According to the sample structure appropriate operation mode is determined[27]. If the correct imaging mode is not chosen sample or cantilever can be damaged.



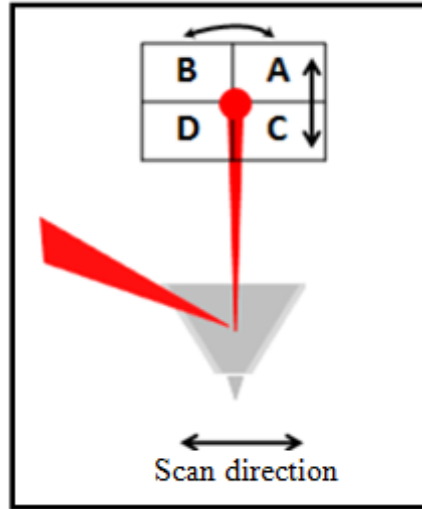
**Figure 2.5 :** Atomic Force Microscope.

Figure 2.6 shows the principle of atomic force microscopy. Atomic force microscopy (AFM) relies on the forces between a sharp tip and sample surface. The tip is attached to the free end of a cantilever (usually, 100-200 microns long). The cantilever deflects because of the interatomic forces between the tip and sample surface atoms and the deflection of cantilever is measured by means of a laser beam [28].



**Figure 2.6 :** Principle of Atomic Force Microscopy.

A laser beam is reflected from the back side of the cantilever. The reflected beam is collected on a photodiode. The photodiode is divided into four parts (Figure 2.7). When the laser is displaced vertically along the positions top (B-A) and bottom (D-C), there exists a deflection because of topography, while if this movement is horizontal left (B-D) and right (A-C), it produces a torsion due to lateral force.



**Figure 2.7 :** Beam Deflection System,Using a Laser and Photodiode to Measure the Beam Position [27].

Piezoceramic materials can expand or contract in the presence of voltage gradient and conversely they develop an electrical potential in response to mechanical pressure. This way, movements in x, y and z direction are possible. This property makes piezoelectric crystals useful in many applications[29].

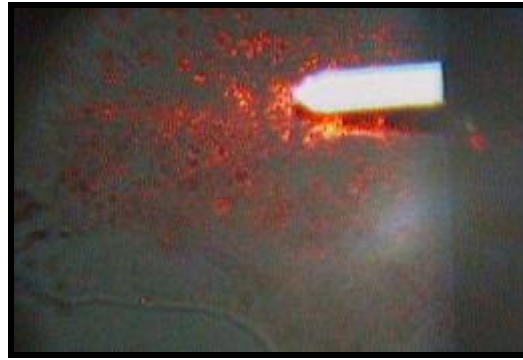
The key component of the atomic force microscope is a cantilever with a tip. The tip must be sharp enough [27] to record with high lateral resolution. The fundamental mechanical parameters in a cantilever for AFM are its resonant frequency, its spring constant and its physical dimensions. The spring constant is defined as the ratio between the force applied at the free end of cantilever and the cantilever deflection at its free end. Typical spring constants [30] are between 0.001 to 100 N/m[34].

To calculate the resonant frequency of a cantilever, one has to solve the equations of motion for the cantilever and find the eigenvalues. The equations of motion are typically partial differential equations and can be solved in closed form in only a few cases. One such case is a rectangular type cantilever, for which the resonant frequency;

$$F_r = \frac{1}{2\pi} \sqrt{\frac{k}{m^*}} \quad (2.1)$$

where k is the force constant and  $m^*$  is equal to 0.24 times the mass of the cantilever[31]. Cantilevers typically range from 100 to 200  $\mu\text{m}$  in length, 10 to 40  $\mu\text{m}$  in width, and 0.3 to 2  $\mu\text{m}$  in thickness. Integrated cantilevers are usually made from silicon (Si) or silicon nitride ( $\text{Si}_3\text{N}_4$ )[31-32]. The tip can be coated different

materials for different applications such as electrostatic force microscopy (EFM), magnetic force microscopy (MFM). They are characterized by their force constant and resonant frequency, which have to be chosen according to the sample to be studied. TAP300-G (Figure 2.8) and PPP-NCHR were used during our dynamic mode measurements.

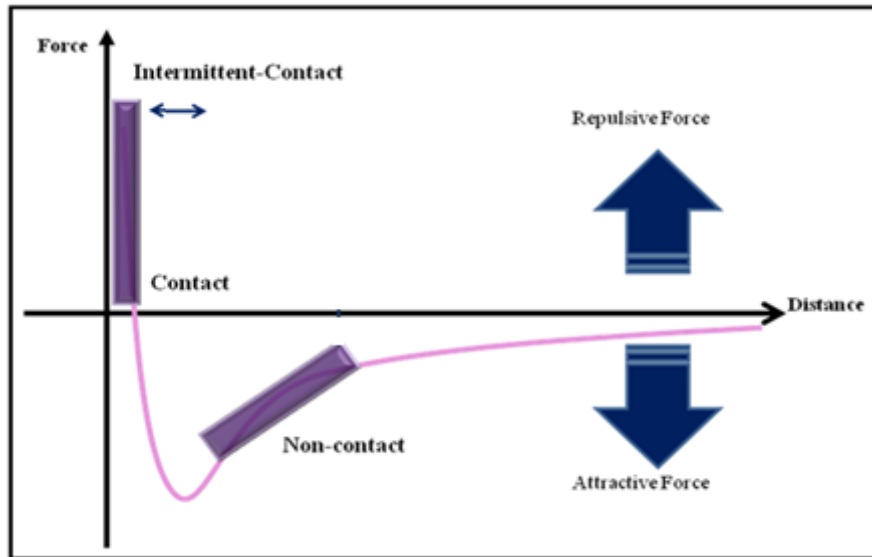


**Figure 2.8 :** AFM Cantilever.

Atomic force microscope works with the forces between the tip and sample[4,19]. The force is not measured directly, but calculated by measuring the deflection of the lever. The cantilever is flexible and behaves like a spring, and knowing the stiffness of the cantilever[31]. Hook's law gives;

$$F = - kz \quad (2.2)$$

where F is the force, k is the stiffness of the lever, and z is the distance the lever is bent. To consider the tip-sample interaction, refer to the interatomic force versus distance curve in **Figure 2.9**. When the tip to sample separation is relatively large, the cantilever is weakly attracted to the sample. With decreasing distance, this attraction increases until the separation becomes so small that the electron clouds of the tip and sample atoms begin to repel each other electrostatically. The net force goes to zero at a distance on the order of the length of a chemical bond (a few Å) and at a closer distance the repulsion dominates.



**Figure 2.9 :** Interatomic Force Versus Distance Curve.

There are three imaging modes in AFM;

- Contact Mode
- Non-Contact Mode
- Intermittent (Tapping or Dynamic ) Mode

#### **2.2.4 Contact mode**

In contact mode, the tip is in physical contact with the sample[27] and the tip-sample separation is on the order of a few Å[25], thus the atomic resolution can be achieved. The force on the tip is repulsive with a mean value of 10 nN[24]. This force is set by pushing the cantilever against the sample surface with a piezoelectric positioning element[21-22]. In this mode, the deflection of the cantilever is sensed and compared in a DC feedback amplifier to some desired value of deflection. If the measured deflection[33] is different from the desired value the feedback amplifier applies a voltage to the piezo to raise or lower the sample relative to the cantilever to restore the desired value of deflection. The voltage that the feedback amplifier applies to the piezo is a measure of the height of features on the sample surface. It is displayed as a function of the lateral position of the sample. Although forces are only of the order of 1nN, the pressure applied to the sample ,can easily reach 1000 bar because the contact area is so small. This may lead to structure damages,especially on soft surfaces. For contact mode, it is necessary to have a cantilever which is soft enough (approximately 0.01 - 10N/m ) to be deflected by very small forces and has



a high enough resonant frequency to not be susceptible to vibrational instabilities[34].

### 2.2.5 Non-Contact mode

In non-contact mode, the tip-sample separation is 50 - 150 Angstrom and the tip is quite close to the sample but not touching it, the cantilever is affected by weak attractive forces[24]. The forces between tip and sample are on the order of pN ( $10^{-12}$  N) In this mode, the detection scheme is based on measuring changes to the resonance frequency or amplitude of the cantilever[24]. The stiff cantilever (20-100N/m) is kept vibrating near its resonance frequency. Typical frequencies are from 100 to 400 kHz, typical amplitude is of a few tens of Å. Due to interaction with the sample, the cantilever resonance frequency  $f_1$  changes according to;

$$f_1 \propto \sqrt{k - F'} \quad (2.3)$$

where  $F'$  is the force gradient and  $k$  is the cantilever spring constant. If the resonance frequency (or vibrational amplitude) is kept constant by a feedback system which controls the scanner height, the probing tip traces lines of constant gradient. The motion of the scanner is used to generate the data set [34].

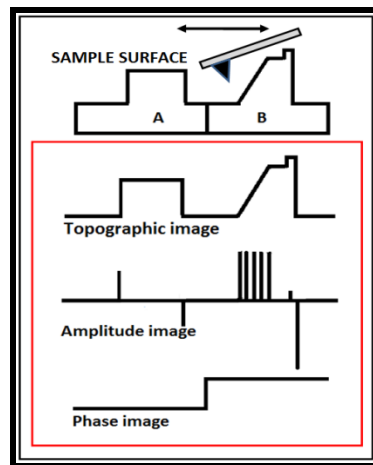
### 2.2.6 Intermittent (tapping or dynamic) mode

The Intermittent (tapping or dynamic) mode is similar to non-contact mode, the only difference that the tip touches the sample periodically[35] and the cantilever is vibrated near its mechanical resonance frequency (300 kHz)[26]. Part of the oscillation extends into the repulsive regime. An electronic feedback loop ensures that the oscillation amplitude remains constant, such that a constant tip-sample interaction[36] is maintained during scanning. Forces that act between the sample and the tip will not only cause a change in the oscillation amplitude, but also change in the resonant frequency and phase of the cantilever. The amplitude is used for the feedback[37] and the vertical adjustments of the piezoscanner are recorded as a height image. Simultaneously, the phase changes are presented in the phase image (topography). Very stiff cantilevers are used in this mode. Intermittent mode does not provide atomic resolution but appears to be advantageous for imaging rough surfaces with high topographical corrugations. During the all experiments, intermittent mode was used [34].

### 2.2.7 Phase imaging

Phase imaging shown in Figure 2.10 is not really an operation mode in itself and applied in dynamic mode[36]. It is used to image qualitative distinction in sample composition with high spatial resolution[38]. The measurement of the difference in phase angles between the excitation signal and the cantilever response is used to map compositional variations in heterogeneous samples[36,39]. Imaging phase changes is an effective tool for sharp topographic changes in rough surfaces for imaging heterogeneous samples. Despite its wide experimental use, how to interpret height and phase contrast images in term of the sample properties is still open[39].

Several models have been developed to describe the nature of the phase contrast and have demonstrated its dependence on multiple factors, including tip and sample elasticity, adhesion, tip size and shape and other surface forces. In 1996 Garcia and Tamayo suggested that the phase signal in soft materials is sensitive to viscoelastic properties and adhesion forces [40], with little participation by elastic properties.



**Figure 2.10 : Phase Imaging.**

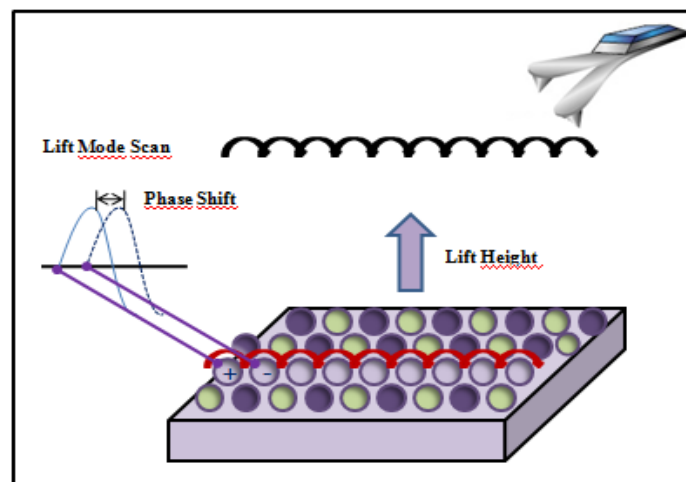
### 2.2.8 Electrostatic force microscopy

The electrostatic forces on a conducting cantilever depend on the nanoscale electrical properties of the sample below it [41]. In electrostatic force microscopy (EFM), these electrostatic interactions are used in order to measure the local charge, dielectric constant, and work function of the sample [41-42]. The strength of the electric interaction between the tip and sample is adjustable in EFM by applying a voltage between the tip and sample [43-44]. In EFM measurements cantilevers must be

conductive coated [37]. Tips are coated with a thin ( $< 50\text{nm}$ ) conductive film such as Cr/Pt.

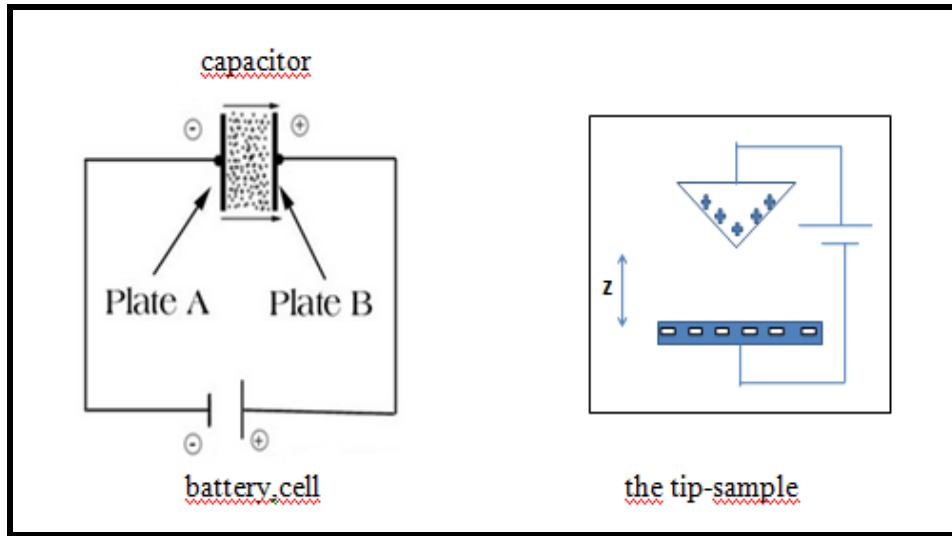
Electrostatic force microscopy (EFM) is a version of AFM and a secondary imaging mode [42] derived from dynamic mode. Contact mode, intermittent mode and non-contact mode scanning probe microscopy use short range van der Waals forces to probe the topographic features of a sample. However, if we move the cantilever further away from the surface ( $\sim 60\text{-}100\text{nm}$ ), we can examine longer range forces [37,44], such as magnetic and electrostatic forces [42,44].

We can learn about the electrical properties of a material with high spatial resolution [42,44]. Van der Waals forces and electrostatic forces have different dominant regimes. Van der Waals forces are proportional to  $1/r^6$ , while electrostatic forces are proportional to  $1/r^2$ . Thus, when the tip is close to the sample, van der Waals forces are dominant. As the tip is moved further away from the sample, the van der Waals forces rapidly decrease and the electrostatic forces become dominant. Forward scan is used for to determine the topography [37], while the backward is used to determine electrostatic state in the lift off mode. In the lift off mode [42], the first scan is performed to obtain the topography by scanning the tip near the surface. In the second scan, system lifts the tip and increases the tip-sample distance in order to place the tip in the region where electrostatic forces are dominant [37]. A voltage is applied between the tip and sample and it is scanned without feedback, parallel to the topography line like in Figure 2.11.



**Figure 2.11 :** Principle of Electrostatic Force Microscope.

To understand EFM, we can think a capacitor[43];



**Figure 2.12 : Capacitor.**

Capacitors[42] store electrical energy. Inside the capacitor (Figure 2.12), the terminals connect to two metal plates separated by a non-conducting substance, or dielectric. When there is a potential difference (voltage) across the conductors, a static electric field develops across the dielectric, causing positive charge to collect on one plate and negative charge on the other plate. Energy is stored in the electrostatic field. Energy stored on a capacitor;

$$C = \frac{Q}{V} \quad (2.4)$$

$$U = CV^2 \quad (2.5)$$

$$F = -\frac{dU}{dz} = -\frac{d}{dz}(CV^2) = \frac{dC}{dz} V^2 \quad (2.6)$$

where  $U$  is the potential energy,  $C$  and  $V$  are capacitor and voltage.

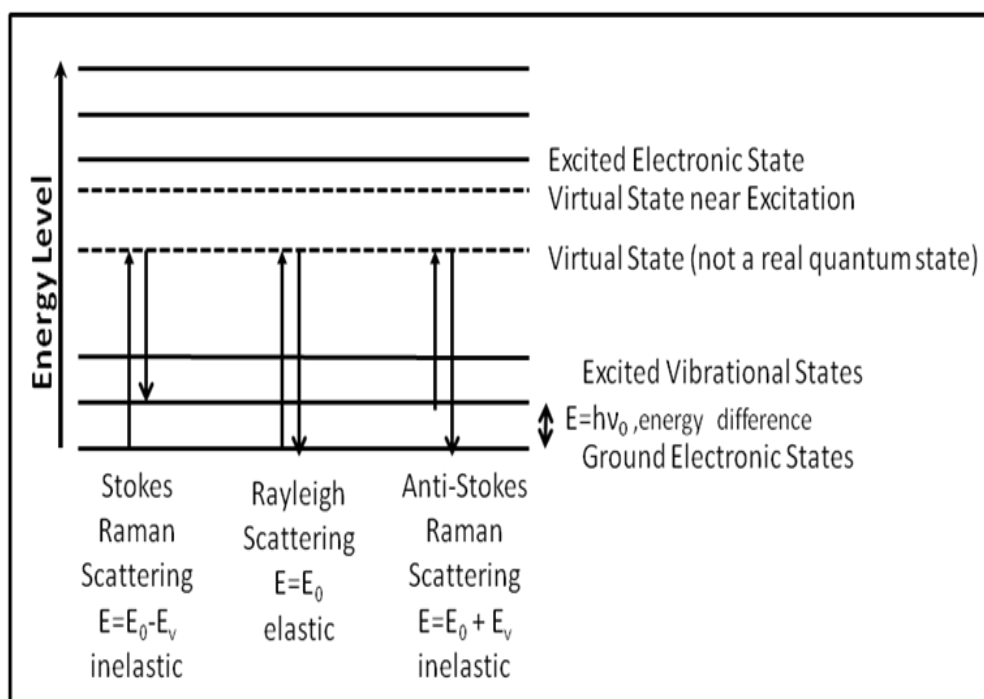
$\frac{dC}{dz} < 0$  force is always attractive.

### 2.2.9 Raman microscopy

Raman spectroscopy is a very useful and powerful characterization method[45-48] for aqueous, gaseous and solid systems. It is used in the qualitative and quantitative analysis of the compounds [49]. Chandrashekhara Venkata Raman discovered the inelastic scattering of light (Raman effect) in 1928 and he won Nobel prize in 1930

[49-50]. In the inelastic scattering, energy and frequency of photons in light source changes interaction with a sample.

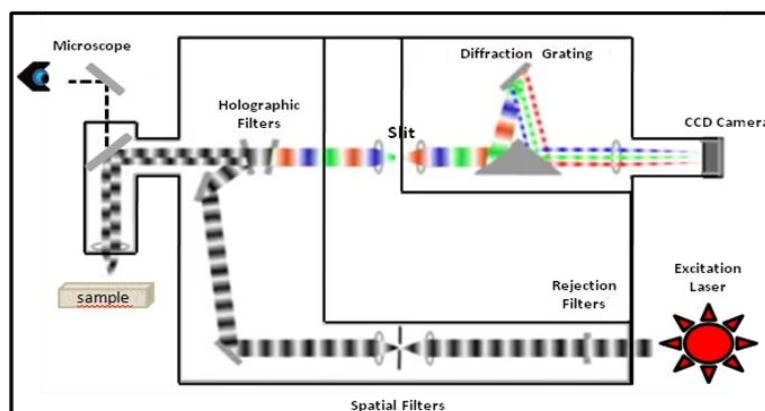
Raman spectroscopy uses a laser in order to excite the molecule or other compound structures on the surfaces or in a crystalline system [50-51]. There are three options for the incident photons; they will be absorbed, transit the material without interaction or scattered and Raman uses the light scattering. There are two types scattering in the visible light and near infrared range; Rayleigh and Raman scattering[51]. Figure 2.13 shows the energy diagram for Rayleigh scattering and Raman scattering processes.



**Figure 2.13 :** Energy diagram for Rayleigh and Raman Scattering [49,51].

In Stokes scattering; molecule absorbs photon and jumps to virtual state from the ground state then emits photon. The frequency of the scattered light decreases when compared to the frequency of the incident photon. In Rayleigh scattering; molecule absorbs photon and jumps to virtual state. The frequency of the scattered light does not change when compared to the frequency of the incident photon. In Anti-Stokes scattering; molecule starts in a vibrational state on account of prior excitation or thermal perturbation. Molecule absorbs photon and jumps to virtual state, emits a photon. The frequency of the scattered light increases when compared to the frequency of the incident photon [49,51].

In Raman spectroscopy, the difference in energy between the excitation source and the scattered light tells us the energy of a vibrational state of the scattering molecule (or a phonon of the system) [46, 50-51]. The measurable difference in wavelength is named as the Raman shift. A Raman spectrum plots Raman intensity (number of scattered photons collected) versus the difference in wavenumber from the excitation wavelength. The Raman intensity is proportional to  $1/\lambda^4$  [52-53], namely short excitation source wavelengths give a much stronger Raman signal. Pattern of all peaks gives the chemical fingerprint. Raman scattering is a very weak process [54]. One in every  $10^7$  photons is scattered inelastically [46,51]. Vibrations of multiply bonded or electron rich groups create more intense Raman bands when compared with vibrations of single bonded or electron poor groups [50]. A Raman spectrometer consists of a monochromator, detector, excitation source and sample holder [49]. Raman shifts of the quantum dots were measured by Renishaw Raman Microscope. In Figure 2.14 a typical Raman spectroscopy system is shown.

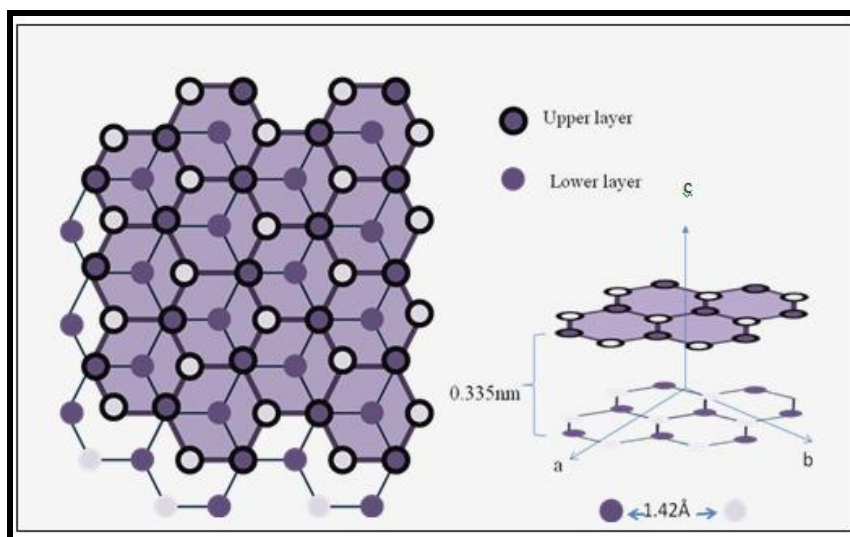


**Figure 2.14 :** Raman Spectroscopy System [55].

## 2.3 Substrates

### 2.3.1 Highly oriented pyrolytic graphite (HOPG)

A carbon atom has six protons and consequently six electrons ( $1s^2 2s^2 2p^2$ ). Several carbon allotropes are found in nature; graphite and diamond. Graphite is formed by layers of honeycomb atomic array of carbon atoms with interatomic distance of 1.42 Å and the distance between planes is approximately 0.335 nm. Graphite is hydrophobic [56]. A single layer of graphite is called graphene. While the carbons within a sheet are covalently bonded to form hexagonal lattice structure (Figure 2.15), the layers are held together by Van der Waals forces [56].



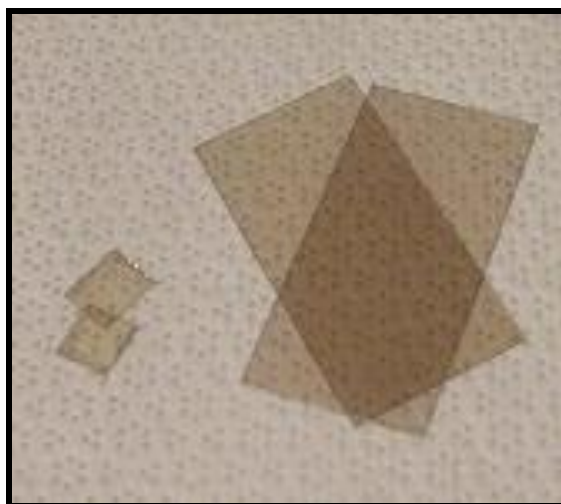
**Figure 2.15 :** The Structure of The Bulk Hexagonal Graphite Crystal.

Highly oriented pyrolytic graphite (HOPG) is an artificial graphite and synthesized from carbon rich gases, decomposed and adsorbed onto a surface (pyrolysis), subsequently heated to high temperatures (approximately 3000 K) under high pressure (several atmospheres). After 500°C it starts to burn in air. The fabricated material consists of large graphitic domains (several  $\mu\text{m}$ ) with an angular variation of the c-axis direction of less than one degree, hence the term highly oriented [57].

HOPG has a renewable and smooth surface. Unlike mica, HOPG is completely non-polar and conductor. It is being used as calibration references in scanning probe microscopy (SPM) and it is easily cleaned by scotch tape, take a piece of tape, press it onto the flat surface [40], pull it off and take a thin layer of HOPG. There are approximately 20-40 cleavings per sample. We use grade SPI-2 HOPG [57].

### 2.3.2 Mica

Mica is an important and useful mineral that has become a standard substrate, due to its easy cleavage [58]. Its chemical formula is  $\text{K}_2\text{O} \cdot \text{Al}_2\text{O}_3 \cdot \text{SiO}_2$ . The cleaved sheets (in Figure 2.16) have good optical clarity, the higher the transparency being associated with the higher the quality of the mica and they could be observed at the atomic or near atomic scale with AFM. The structure of mica forms layers and these sheets are chemically inert, elastic, flexible, reflective, refractive, flat, hydrophilic, insulating, lightweight. Mica is a dielectric materials and therefore, on its own, can not hold a charge [59].



**Figure 2.16 : Mica Sheets.**

### **2.3.3 Gold on mica (Au 111)**

Mica sheets can be coated by gold like in Figure 2.17. The substrates were prepared by sublimation of gold on mica[40]. The sublimations were carried out in a vacuum chamber with pressure of  $10^{-7}$  Torr. Freshly cleaved mica sheets were pre-heated in order to degas environmental impurities. Then, 150nm of gold were deposited with the mica substrate and the substrate was cooled down to room temperature. By this method, atomically flat Au (111) substrates. The triangular shape of the Au (111) surface can be clearly seen via AFM.



**Figure 2.17 : Gold on Mica**



## **2.4 Solvent**

### **2.4.1 DI water**

Natural water is not pure. There are some contaminants inside it and these contaminants can affect our results in a negative way. One way to remove these contaminants from water is to boil it until it changes to steam, a process known as distillation. When this steam is allowed to cool down and condense into liquid form again, the result is a purified form called distilled water. Distilled water should ideally be nothing but hydrogen and oxygen molecules, with a PH level of 7 and no additional gases, minerals or contaminants. Distilled water was used to preparation of DNA samples. In this study, Merck Water for chromatography LiChrosolv® and VWR were used. In addition, we bought a water system in order to produce our pure water from ELGA (which produces Type-II ultra plus water with TOC less than 2 ppb).

### **2.4.2 Toluene**

Toluene is a clear, colorless liquid with a distinctive smell. Molecular formula of the toluene is  $C_7H_8$ . It is added to gasoline along with benzene and xylene. It is an aromatic hydrocarbon. Toluene is remarkable solvent for quantum dots.



### 3. INVESTIGATION OF SOLVENT EFFECT

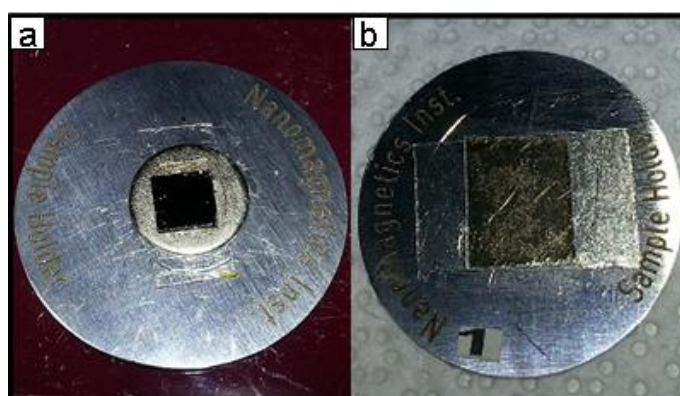
#### 3.1 Experiments

##### 3.1.1 Water effect on HOPG and mica

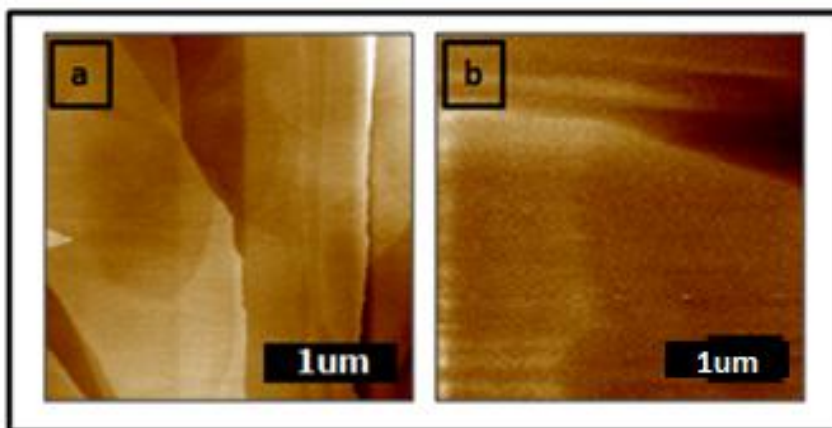
Sample surfaces are called hydrophilic or hydrophobic according to attraction at the solid-liquid interface. If the molecules of a liquid are strongly attracted to the molecules of a solid (adhesion) then a drop of the liquid will completely spread out on the solid surface so better adhesiveness and higher surface energy. These surfaces are called hydrophilic surfaces. Unless the molecules of liquid are strongly attracted to the molecules of a solid, namely attraction is weak, lower surface energy then the surface is called hydrophobic. If the surface is hydrophobic, when you drop on water the droplet will stay intact on the surface. HOPG and gold[40] are hydrophobic substrate, but muscovite mica is hydrophilic surface[56, 60-61].

While the DNA samples are prepared, the water is used as a solvent. During the experiments DNA solutions were dropped on the hydrophilic and hydrophobic surfaces. Water effect on these different surfaces is very important to our results.

In Figure 3.1 hydrophobic HOPG and hydrophilic mica surfaces are seen. Before drop the water on these surfaces, they were investigated using AFM.



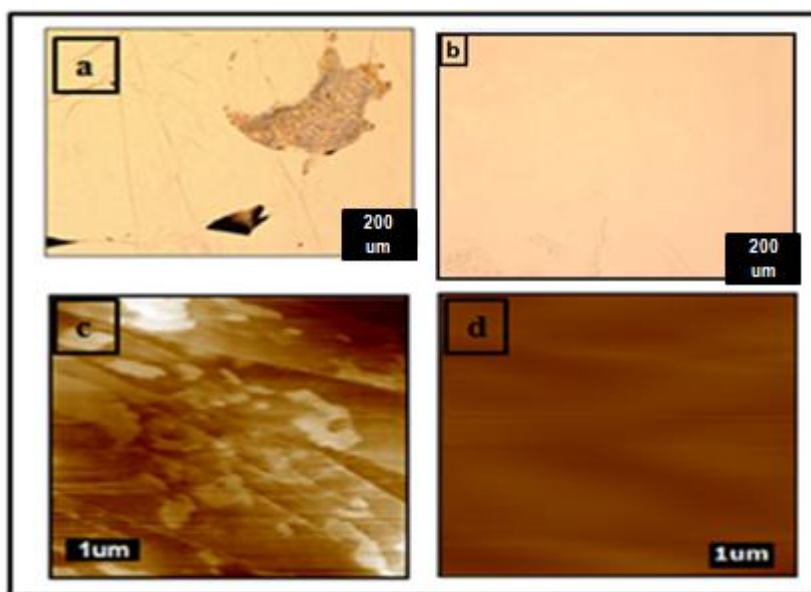
**Figure 3.1 :** Hydrophobic and Hydrophilic Surfaces.



**Figure 3.2 :** (a) HOPG-13 and (b) Mica Surface

In Figure 3.2, AFM images of HOPG and mica are seen, namely topography of these surfaces. As the dark sides show the low areas, the bright sections show the high areas. Both HOPG and mica are flat surfaces. In the AFM image of HOPG (a) steps are seen.

1  $\mu$ L DI (Merck) water was dropped on HOPG and mica surfaces and these surfaces were observed by atomic force microscope. In the mica surface, the water droplet quickly dried in a few minutes but in HOPG, the water droplet stayed intact on the surface. Figure 3.3 shows the optical microscope images of HOPG-13(a and b) and dynamic mode AFM images of HOPG-13 and mica after drop the water (c and d).

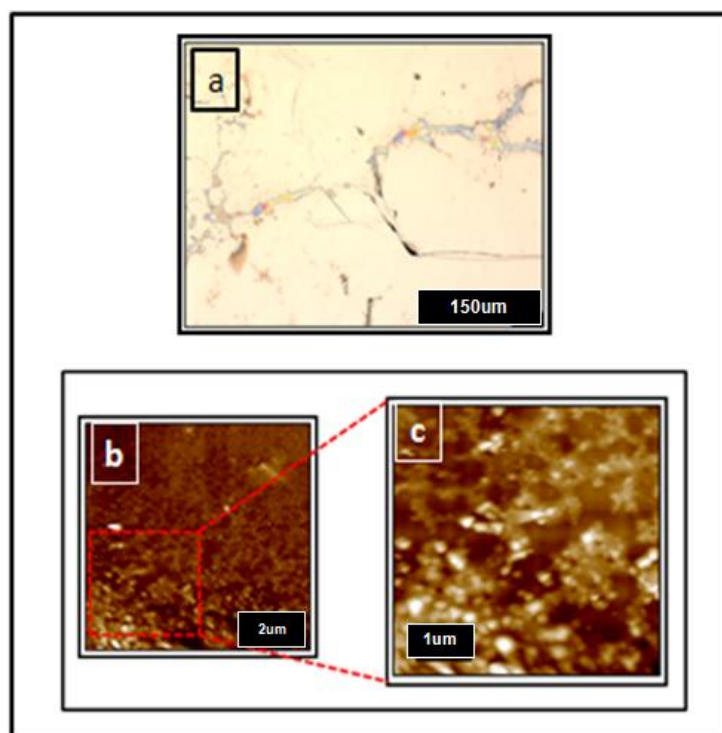


**Figure 3.3 :** (a), (b); Optical Microscope Images, (c) AFM - Merck Water on HOPG-13,(d) AFM - Merck Water on Mica.

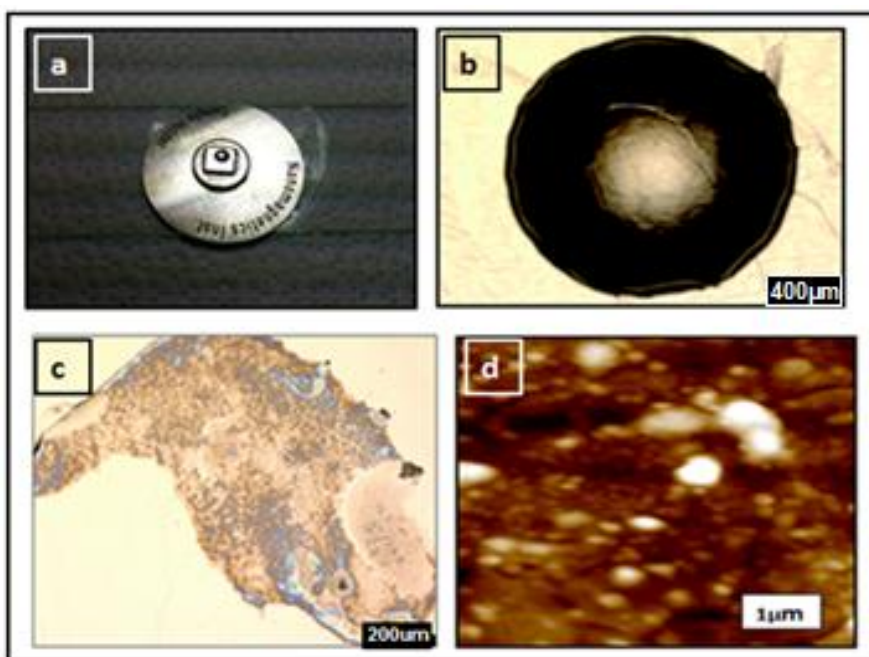
AFM images reveal the formation of the some unexpected structures on the HOPG surface after DI water is dropped on the surface. As if HOPG surface is swelled. There is not any difference on mica surface between before and after dropped the water. After this measurement, a different DI water was dropped on the HOPG. In this way, it will be learned that the problem is driven from the Merck water or not.

Sample-357 was prepared with the other water. VWR water was used to investigate (or understand) the differences between the two DI water.

In Figure 3.4, optic microscope image and AFM images of Sample-357 are seen. In the optical image (a) shows the distribution of the water. When the compare the previous data the water distribution is not dense in this image but it can be easily seen. 2 $\mu$ L VWR water dropped on the HOPG and this sample did not dry quickly. When we compared the results, they were indistinguishable from the first experiment, Merck water. The surface was badly influenced from the water.

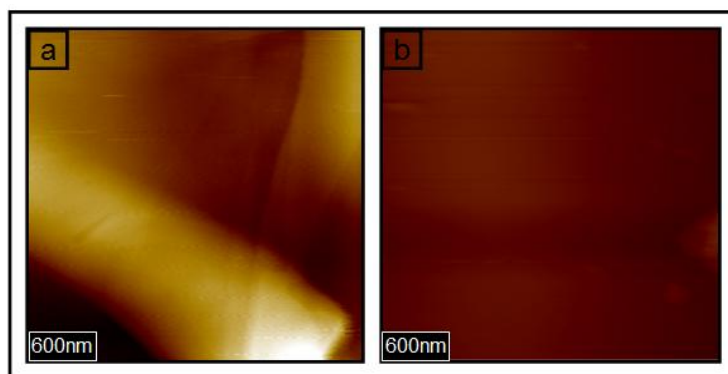


**Figure 3.4 :** Sample-357, 2 $\mu$ l VWR Water Drop Casted on HOPG-13, (a) Optical Microscope Image, (b) and (c) AFM Images of Sample-357



**Figure 3.5 :** Sample-373, 1 $\mu$ L VWR water was drop casted on HOPG-13(a) is HOPG-13 with sample holder, (b) is optical image of Sample-373 after drop casted on water, (c) is optical image of Sample-373 a day later and (d) is AFM image of Sample-373.

Sample-373 (Figure3.5) was prepared with 1 $\mu$ L VWR water. After drop casted the water directly Sample-373 observed via optical microscope and the water droplet can be clearly seen. The result didn't change.



**Figure 3.6 :** (a) Clean HOPG-13 and (b)Sample-468, water drop cased on HOPG-13 using our water system, ELGA.

After a new water system was installed in our laboratory, same procedure was applied using this new source. Before drop casting water, HOPG was cleaned by scotch tape. In Figure 3.6 (a) shows the AFM image of HOPG-13. It is clean and flat. (b) is AFM data after drop castedvthe water. Here there is a very big difference.

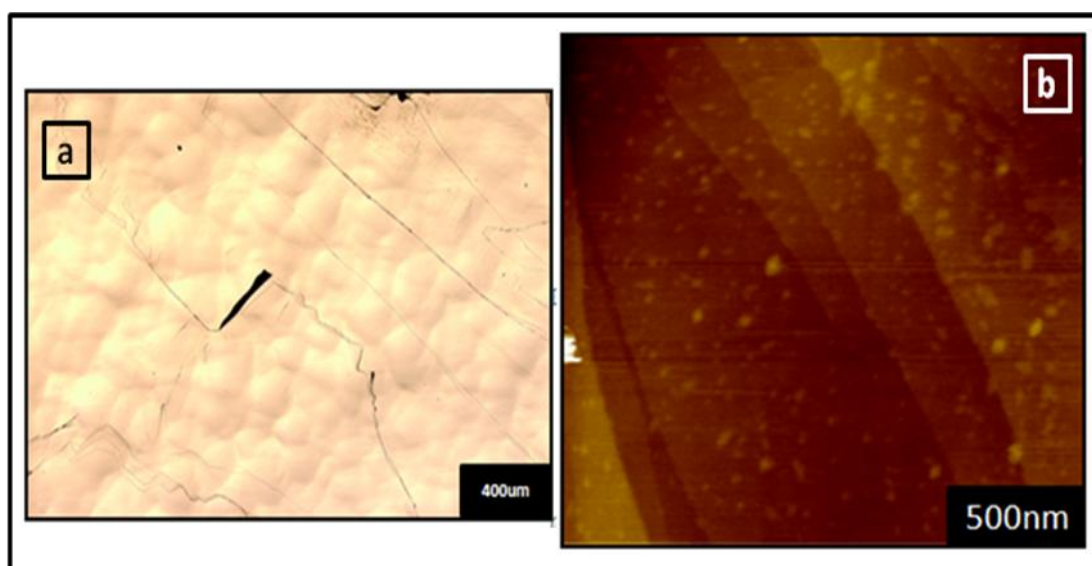
There is some structures on the surface but this is very remarkable when the compare with the other waters.

When the water effect experiments started, there were three kinds water and each one particularly was tried. It was observed that the best water is own water (ELGA) for the measurements.

### 3.1.2 Toluene effect

Toluene ( $C_7H_8$ ) is a clear water-insoluble liquid. Its molecular weight is 92.1384g/mol. Toluene evaporates easily. At room temperature, toluene is a colorless and volatile liquid. It is widely used as an industrial feedstock and as a solvent. Quantum dots are preserved in toluene and they are diluted by toluene. Because of this, toluene effect is an important issue for the quantum dot investigation.

A freshly cleaned HOPG was taken and 1  $\mu$ L toluene drop casted on the surface, Sample-401 (Figure 3.7). As the Figure 3.7 (a) shows the optic image of Sample-401, Figure 3.7 (b) shows the AFM image of Sample-401. Toluene is a volatilized solvent in a few seconds. AFM image of Sample-401 is seen very clearly and steps are apparent. There are small structures on the surface. Toluene did not destroy the surface but sometimes toluene can damage the surface and this can be seen with the naked eye.



**Figure 3.7 :** Sample-401, 1  $\mu$ L Toluene Drop Casted on HOPG-13.





## **4. INVESTIGATION OF CdSe AND InP/ZnS QUANTUM DOTS**

### **4.1 Quantum Dots**

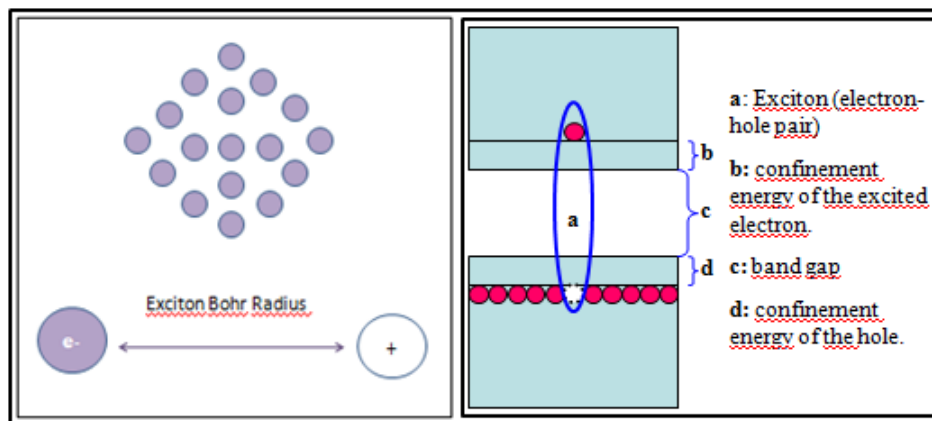
Quantum dot is one of the nanostructures such as tubes, wires. Quantum dots are explained as nanometer-scale semiconductor crystals comprised of groups II–VI or III–V elements[64-66]. Quantum dots (QDs) are very small semiconductor materials which contain tens to a few hundreds of atoms with sizes of a few nanometers[66]. Physical properties of quantum dots strongly depend on crystal size, on account of the quantum confinement effect. First it was realized in 1932 by H. P. Rocksby that the red or yellow color of some silicate glasses could be linked to microscopic inclusions of CdSe and CdS[63]. Such red and yellow colored glasses have been commercially available as color filters for decades. In 1985 Ekimov et al.[67] experimentally proved and theoretically modeled that these changes in color were linked to the density of states (DOS) determined by the size of the crystalline material.

In a semiconductor, electron moves from valance band to conduction band due to light absorption. When energy is introduced to the material, via heat or voltage, some of the electrons are pumped to the conduction band energy level and the excited electron leaves a hole in the valance band [68]. While making the transition from the valence band to the conduction band, the electrons pass through the band gap. The positively charged hole and negatively charged electron may be mobilized via an electric field in order to obtain a current but their lowest energy state is bound electron-hole pair is called an exciton [68].

Electrons in a semiconductor are not stable in the conduction band, so they naturally fall back to the valence band. During this return to the valence band, the absorbed energy is released via electromagnetic radiation. Quantum dots with high luminescent efficiency have attracted attention of researchers due to their wide applications in many fields of science and technology.

#### 4.1.1 The exciton bohr radius

An important feature of the exciton is the so called exciton Bohr radius (Figure 4.1) which describes the average distance between the electron and hole in an exciton[66,68] and it can vary depending on the material. If the size of a semiconductor nanocrystal is smaller than the size of Bohr radius, the charge carriers in a spatially confined and quantum dot's band gap increases since much more energy is needed to confine the exciton[66,68]. Different semiconductors have also different exciton Bohr radius. For instance, the Bohr radius is roughly 9.6nm for the biggest CdSe nanoparticles[68]. This factor is critical to understanding quantum dot behavior. If the quantum dot's size is getting smaller, the absorption and emission wavelengths decrease (shift to blue) and energy increase. If the quantum dot's size increase, the absorption and emission wavelengths increase (shift to red) and the energy decrease.



**Figure 4.1 :** Exciton Bohr Radius.

#### 4.1.2 Quantum confinement

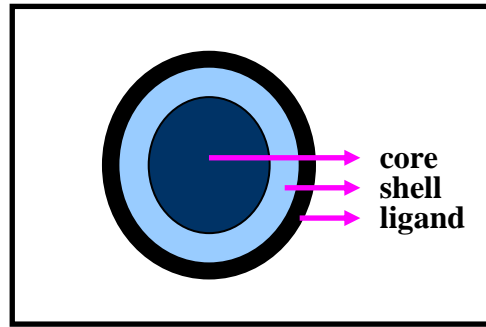
Below a certain size, the properties of the crystalline material start to deviate significantly from bulk properties and became strongly dependent on size. Finite size of the micro crystallites confines the motion of the electron, hole and exciton within their physical boundary. This is called quantum confinement. The degree of confinements is 3D for the quantum dots (Table 4.1). Quantum confinement modifies the density of states (DOS) which in turn leads to discretization as well as enlarged spacing between the energy levels of electron and hole states. Sizes of nanomaterials with dimensions larger than the Bohr radius are described as weakly confined.

Nanomaterials with dimensions smaller than the exciton Bohr radius are strongly confined and possess strongly size dependent behavior.

**Table 4.1 :** Nanostructures, Their Confinements and DOS.

| Structure          | Degree of Confinement | $\frac{dN}{dE}$               |
|--------------------|-----------------------|-------------------------------|
| Bulk Material      | 0D                    | $\sqrt{E}$                    |
| Quantum Well       | 1D                    | 1                             |
| Quantum Wire       | 2D                    | $1/\sqrt{E}$                  |
| <b>Quantum Dot</b> | 3D                    | <b><math>\delta(E)</math></b> |

There are two kinds of quantum dots according to their atomic arrangement in crystal structure such as core types and core-shell types. Figure 4.2 shows the structure of the quantum dot. A core type quantum dot consists of a few atoms. However, a shell of a different material surrounds the core material in core-shell types[65].



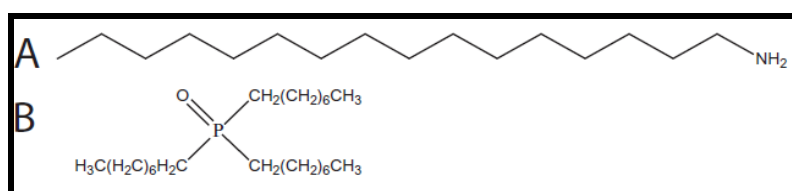
**Figure 4.2 :** Structure of Quantum Dot.

In core-shell types, shell keeps carriers away from the surface. This causes decreasing nonradiative recombination[65] and a great enhancement in optical properties, such as quantum yield and photostability. Electrons and holes are confined to different regions of the structure. In addition, shell is crucial for ligand binding[68]. There are different kinds of core and core-shell type quantum dots such as CdS, CdSe, CdTe, ZnS, CdSe/ ZnS, InP/ZnS. CdSe quantum dots are the most commonly used and investigated quantum dots but to synthesize CdSe quantum dots is not easy. Because higher temperature and pressure is needed and Se precursors are easily oxidized by air. In early studies, Alivisatos produced CdSe by organometallic synthesis method (Alivisatos, et al. 1992). Cadmium selenide has unique optical properties in the visible spectrum [69]. CdSe nanoparticles are used in many research

areas such as biomedical imaging applications, laser diodes, etc. (Alivisatos, et al. 1994, Alivisatos, et al. 1998). InP/ZnS quantum dots are useful[70] and less hazardous alternative to cadmium-based particles. This semiconductor material shows a similar band gap. The core itself is oxidized very rapidly and cannot come in contact with biocompatible solutions without breaking down. Thus, the particles must be capped with a higher band gap material such as ZnS, but differences in the coordination strength between InP/ZnS particles prepared in strong coordinating solvents have unstable shell and a time consuming growth process. InP/ZnS quantum dots are core-shell quantum dots. ZnS is a capping shell, which could act as a potential barrier for photogenerated electrons and holes. Band gap of the InP is 1.34 eV and ZnS is 3.7 eV [71-72].

## 4.2 Experiments

In this section, preparation of the samples on the different surfaces using CdSe and InP/ZnS quantum dots, dispersion of the quantum dots on the surfaces, imaging the samples using atomic force microscope and prepare the samples for photon STM will be discussed. In this study, the CdSe and InP/ZnS quantum dots which are purchased from Sigma-Aldrich were used. The ligand of quantum dots is Hexadecylamine and TOPO (Figure 4.3)[73].

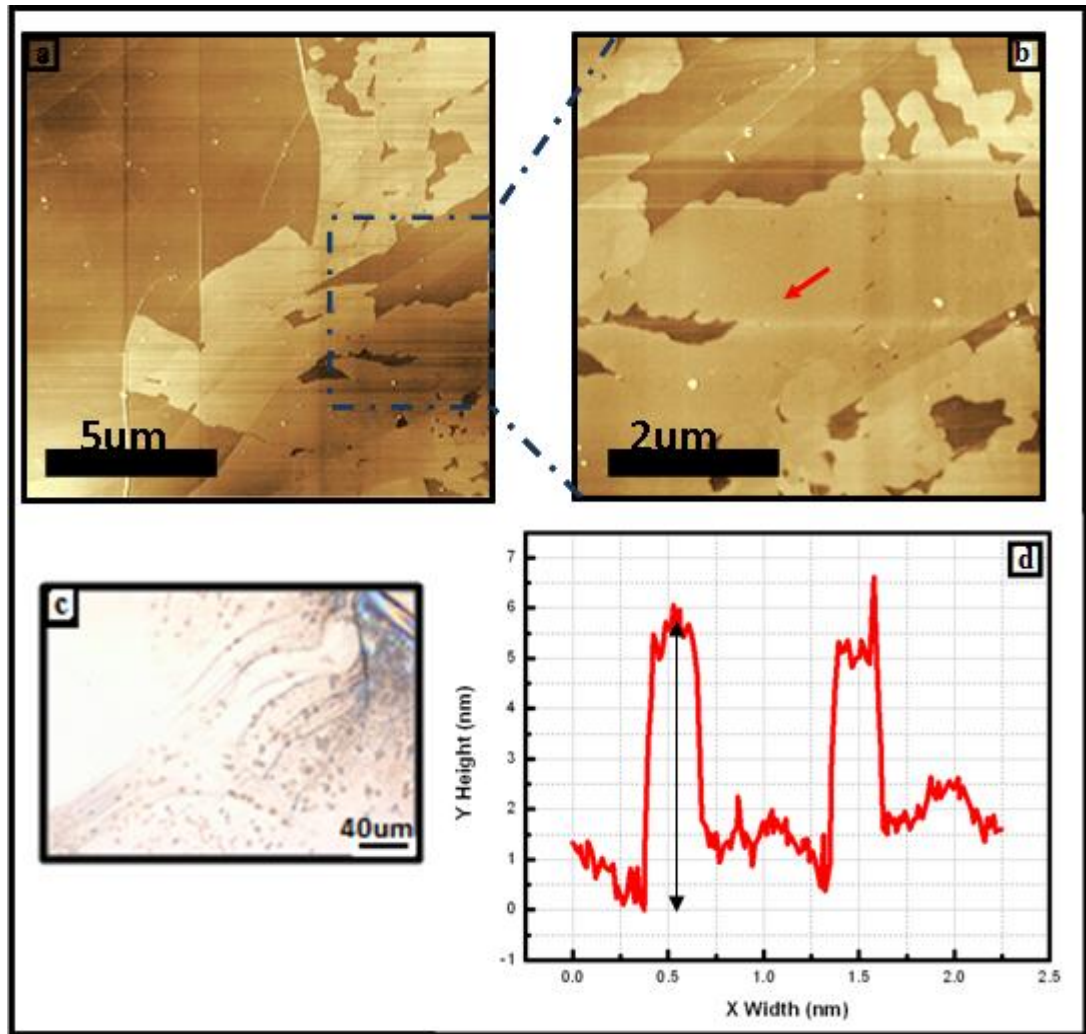


**Figure 4.3 :** Ligands of CdSe Quantum Dots. Ligand A; Hexadecylamine (HDA) and B; Tri-Octylphosphine Oxide (TOPO).

**Table 4.2 :** Properties of CdSe Quantum Dots 640nm Sigma Aldrich

| Properties    | Values                   |
|---------------|--------------------------|
| Type          | CdSe                     |
| Colour        | Deep Red                 |
| Form          | Dispersion               |
| Concentration | 5mg/mL in toluene        |
| Fluorescence  | $\lambda_{em}$ 635-645nm |
| UV absorption | 615-625nm                |
| Particle size | ~ 6.6nm (diameter)       |

Table 4.2 shows the properties of CdSe quantum dots. Their particle size is approximately 6.6 nm. If the ligand is considered, CdSe quantum dots become 10nm. CdSe quantum dots are in toluene and its density 5mg/mL. 1 $\mu$ L of the solution contains  $6.061 \times 10^{12}$  QDs (see Appendix 1). Sample area is 5x5 mm<sup>2</sup>. If 1 $\mu$ L QD solution is drop casted on this area, number of quantum dots per unit area can be calculated. The numbers of quantum dots in 1 $\mu$ L quantum dot solution proportion to sample area and  $2.4 \times 10^{-1}$  QDs are obtained in 1nm<sup>2</sup>.

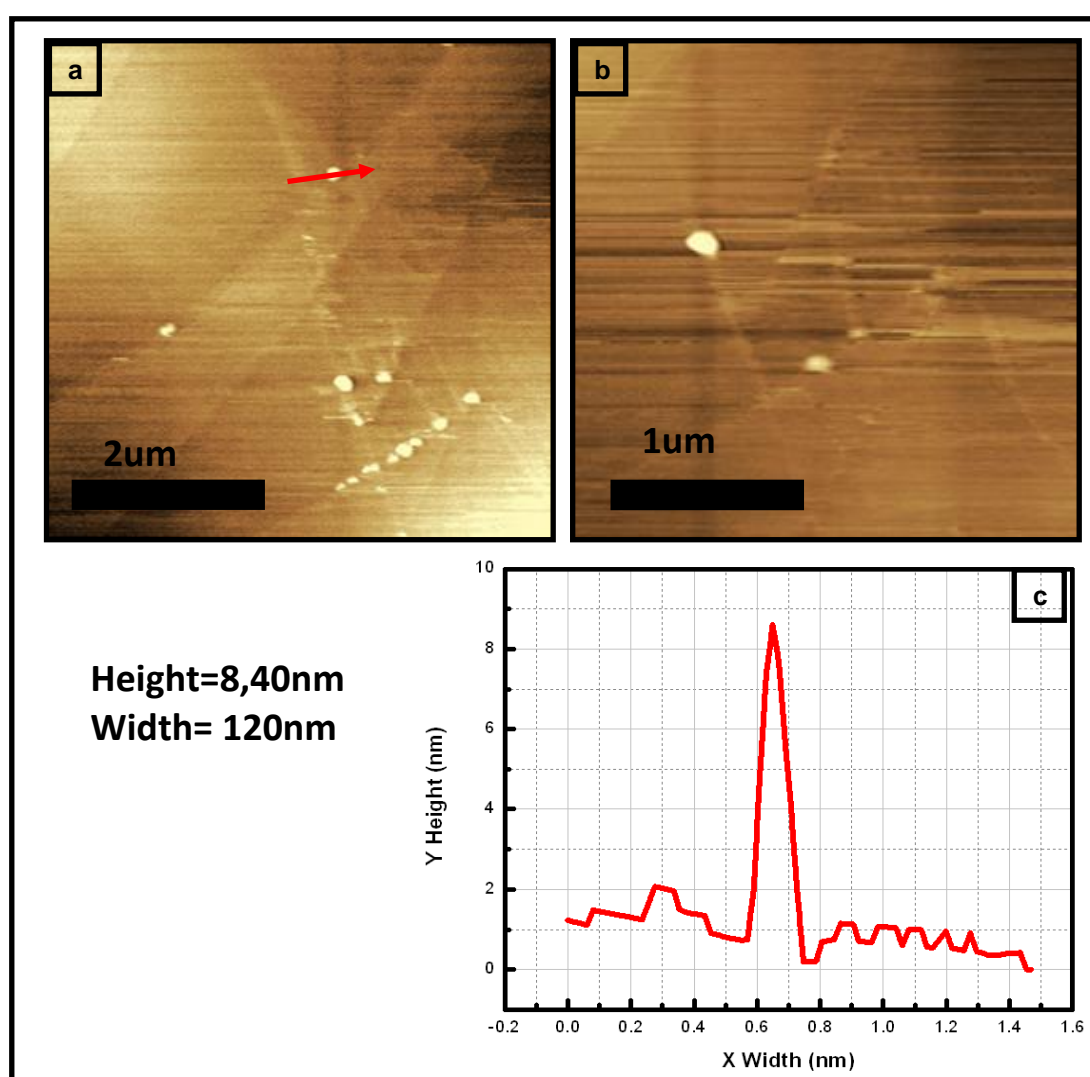


**Figure 4.4 :** (a),(b) AFM Images (c) Optic Microscope Image,(d) height profile of the Sample-300.

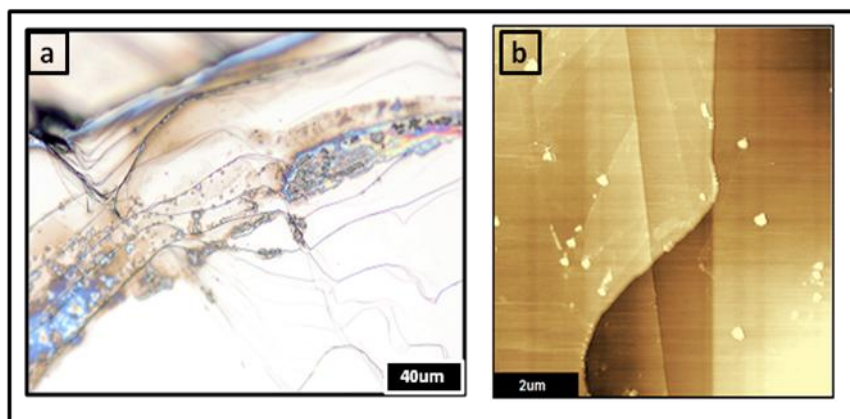
For Sample-300, the first step was to transfer the 2.5  $\mu$ L CdSe QD from their original bottles into the tube and 5000 $\mu$ L toluene was added into the tube, so QD solution was prepared. 1 $\mu$ L from this solution was taken with a micropipette and it was drop casted on HOPG-9 at room temperature. After the dispersion of the quantum dot

solution on the surface, sample was observed by optical microscope and then Sample-300 was placed in desiccators to dry. The optical image(Figure 4.4(d)) shows that QD solution generally is collected at the edge of the surface (or is this the toluene effect). In Figure 4.4 (a) and (b) shows the AFM image of Sample-300. As if a film formed on the surface. Height of this film is approximately 20nm. Besides this, quantum dot clusters are seen on the surface (on the film). Height of the particles  $\sim 5.08\text{nm}$  and with is 70nm, so they are clusters.

In Figure 4.5 shows the same sample but different area. Scan area in (a) is  $5 \times 5 \mu\text{m}$  and (b) is  $2.5 \times 2.5 \mu\text{m}$ .

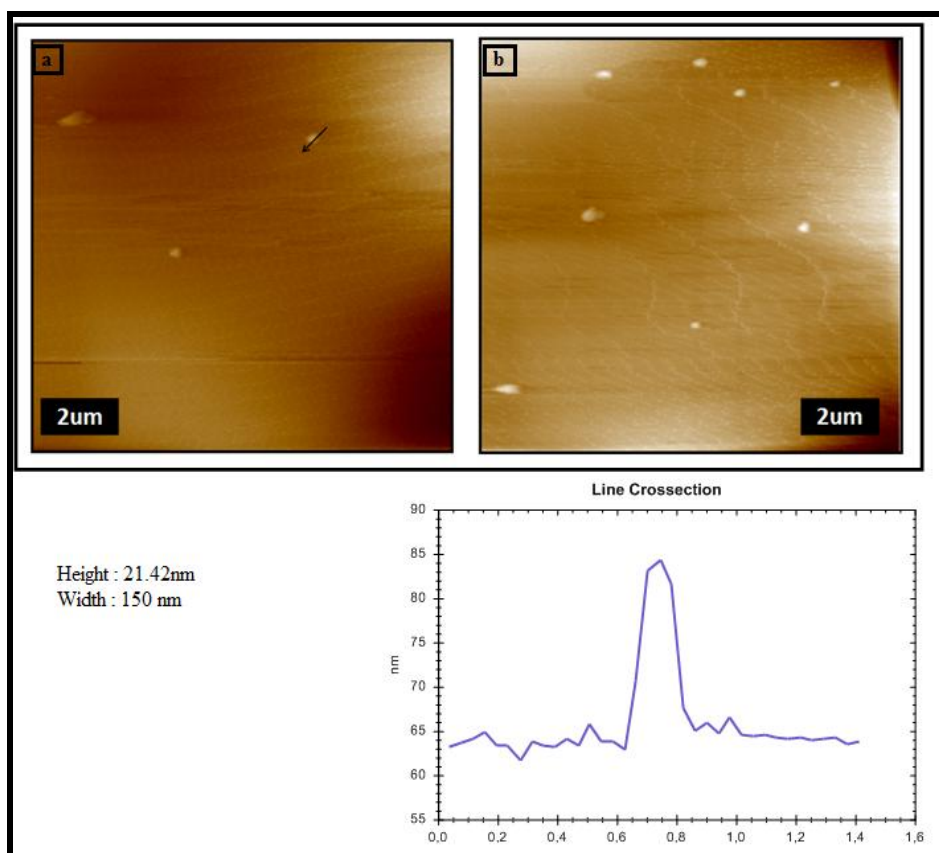


**Figure 4.5 :** (a), (b) AFM Images of Sample-300 in Different Area, (c) Height of Sample-300.



**Figure 4.6 :** Sample-338 , (a) is optical image and (b) is AFM image. 1 $\mu$ L QDs Solution (Diluted by 2.5/5000 with Toluene) Drop Casted on HOPG-9 Surface.

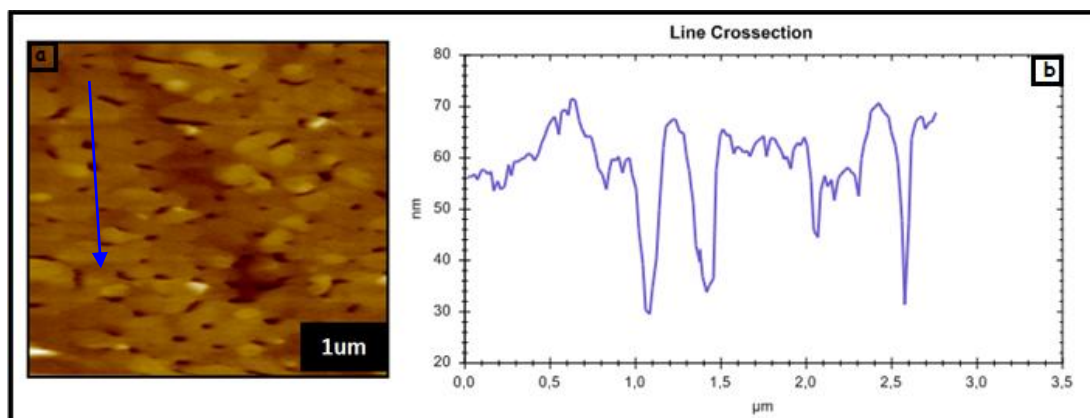
Sample-338 was prepared using the same surface and same quantum dot. 1 $\mu$ L QD solution (diluted by 2.5/5000 with toluene) was dropped on the clean HOPG surface. In the Figure 4.6 (a), QD solution can be seen easily in optical image and in (b) AFM image. HOPG steps are seen and QD clusters. They are not dense. Height of these particles is  $\sim$  13nm.



**Figure 4.7 :** Sample-354, 1 $\mu$ L QDs Solution (Diluted by 2.5/7000 with Toluene) Drop Casted on Cleaved Mica Surface.

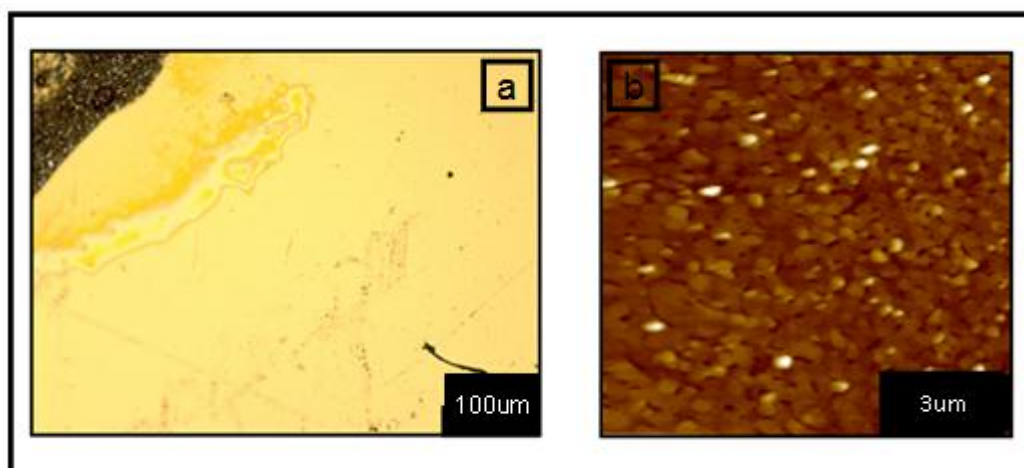


Until this sample, the same surface and the same diluted ratio were used. At this point some modifications were done. Cleaved mica was used instead of HOPG. Sample-354, 1  $\mu\text{l}$  QDs solution (diluted by 2.5/7000 with toluene) drop casted on freshly cleaved mica surface. Mica is a quite flat and quantum dots can be easily seen on it. Figure 4.7 shows the two different area in the same sample. Height of these clusters is  $\sim 22\text{nm}$ . Although the diluted ratio was increased in this solution, particle size also increased. They should be roughly  $\sim 10\text{nm}$ .



**Figure 4.8 :** Sample-375, Gold on Mica (Au 111).

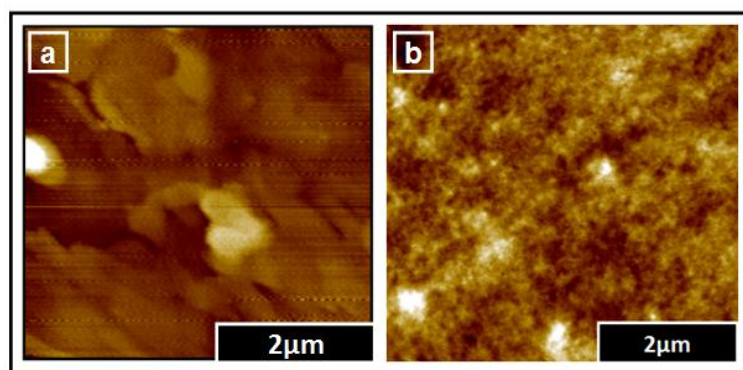
Sample-375 is a 150 nm thick gold film on mica. Hydrogen flame annealing was used on it in order to obtain more flat surface. Gold has a complicated granulated structure. In Figure 4.8 (a) gold surface structure and in (b) height profile can be seen.



**Figure 4.9 :** Sample-380, 1  $\mu\text{l}$  CdSe QD Solution (Diluted by 2.5/5000 with Toluene) Drop Casted on Flat Gold (Au 111) Surface (Sample-375). (a) Optical Microscope Image of Sample-380, (b) AFM Image of Sample-380.

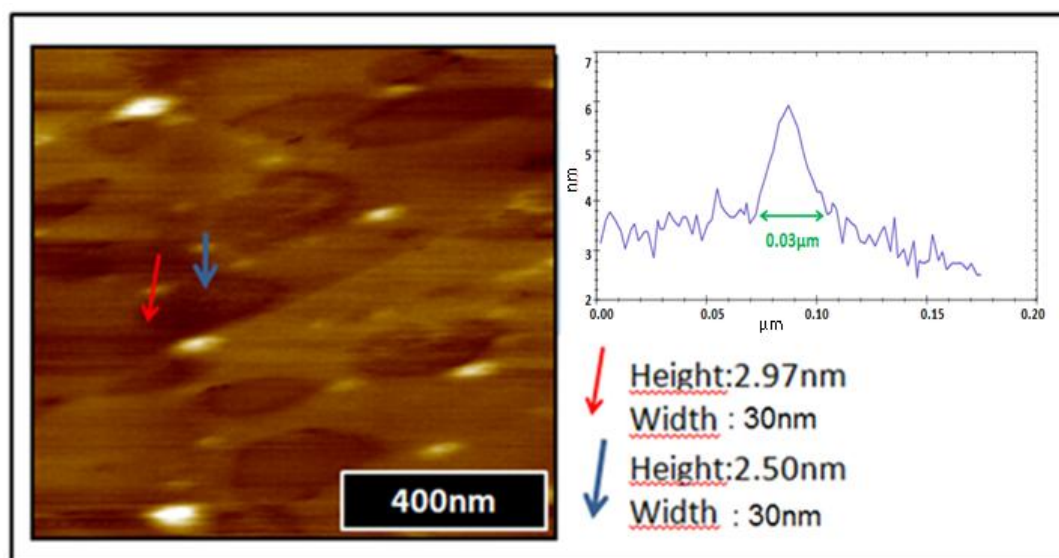


Sample-380(Figure 4.9), 1 $\mu$ L CdSe QD solution (diluted by 2.5/5000 with toluene) drop casted on flat gold (Au 111) surface (Sample-375). This gold surface is well known because previously its topography image was taken with AFM. When the looked at the Sample-375 and the Sample-380, there isn't certain difference between the two samples. It is ambiguous that the small particles are quantum dots or not.



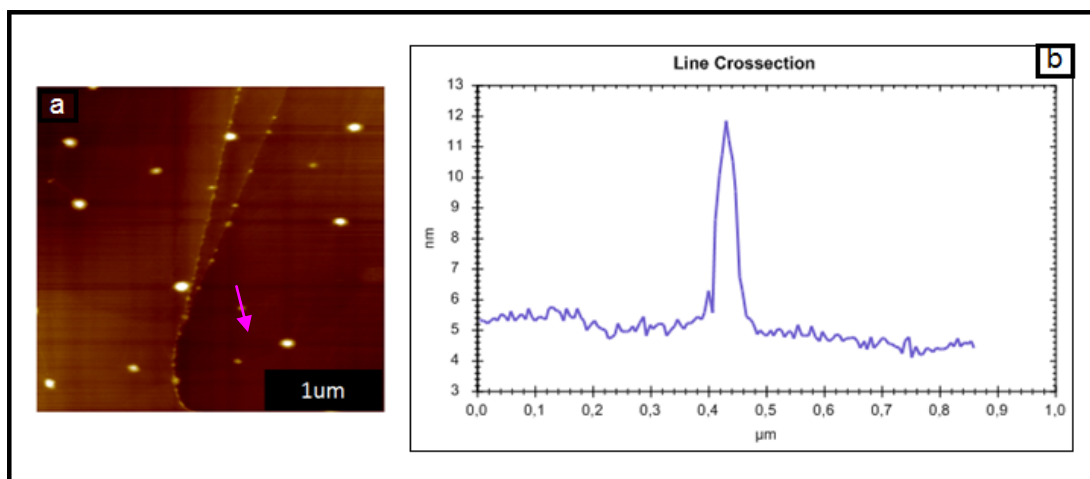
**Figure 4.10:** Sample-392 (Gold Coated Mica), (b) Sample-398, 1 $\mu$ L CdSe QD Solution (non-diluted) Drop Casted on Sample-392.

Before the Sample-398, QD solution was diluted with the solvent toluene. Figure 4.10 (b) shows the not diluted sample. If the QD solution was not diluted with toluene this is practically what is observed. QDs clusters (bright sections) can be seen on the surface. When the solution was diluted, the result was not clean cut.



**Figure 4.11:** Sample-393, 1 $\mu$ L QD Solution (Diluted by 2.5/5000 with Toluene) Drop Casted on HOPG-9, There are Stains on the Surface.

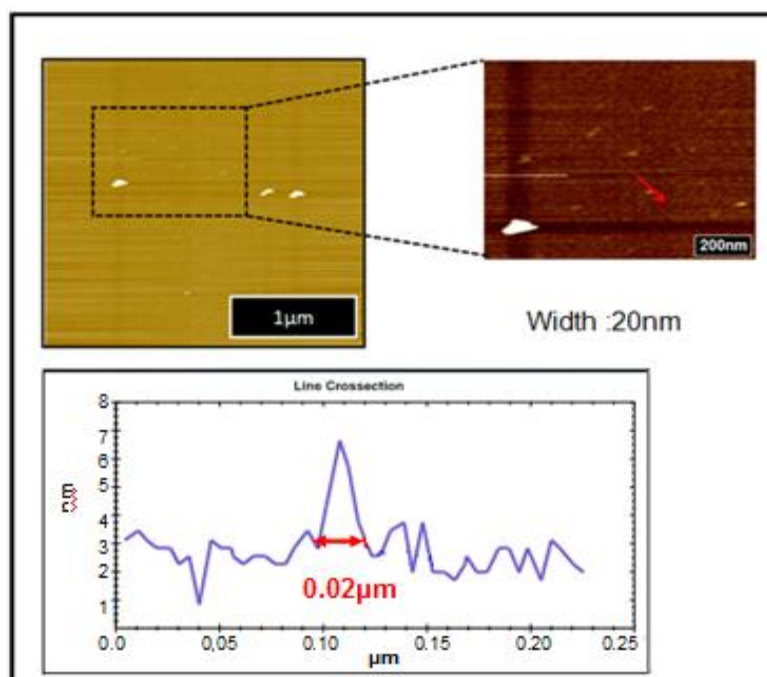
Sample-393 In Figure 4.11 was the sample prepared on the HOPG surface. There are small particles in here and their heights are approximately ~3nm and their widths are ~ 30nm. Widths are very big in comparison with heights. There are some stains on the surface. This situation has never existed before in Sample-338 or Sample-354. This can be driven from QD solution (TOPO ligands) or toluene. Toluene was the fresh. Toluene is suitable as it intercalates into HOPG layers. This sample was annealed in order to understand the reason of these stains.



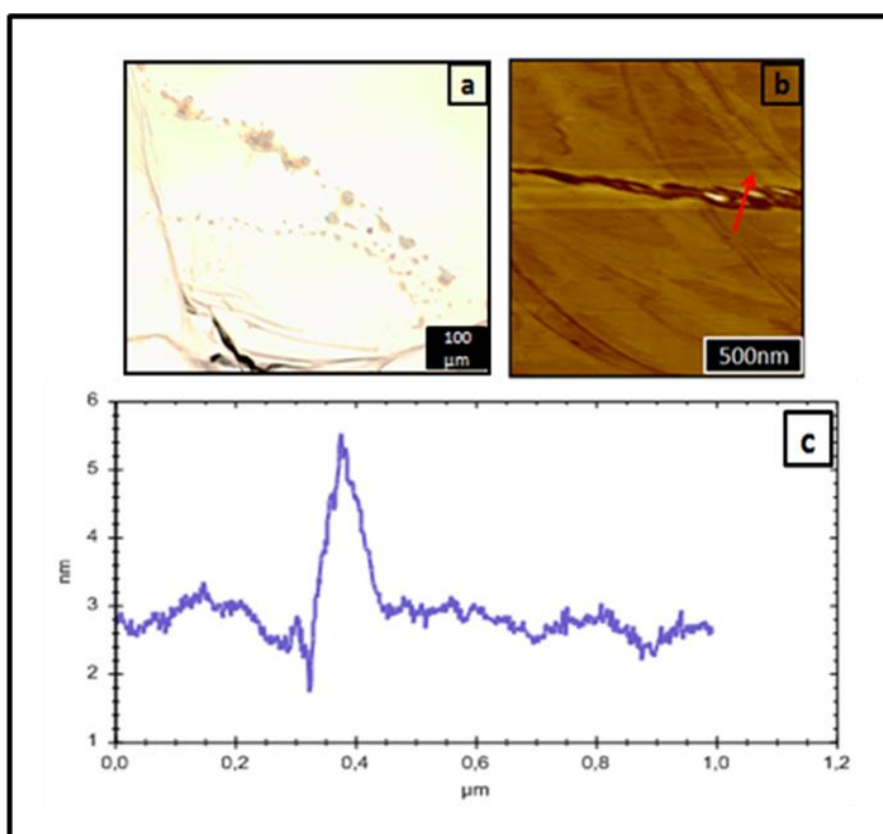
**Figure 4.12:** (a) Sample-411 and (b) height profile of Sample-411.

Sample-393 was annealed get rid of the stains under  $H_2 - Ar$  atmosphere, 120 °C and 1h. All of the strains and contaminants disappeared by means by annealing. As can be seen in Figure 4.12, quantum dots are accumulated at the HOPG steps. HOPG step size is 2.05nm so it consists 6.1 steps. Height of these clusters (b) is ~6.5nm. Before annealing heights of the particles were approximately ~3nm.

Sample-408, 1 μl CdSe QD solution (diluted by 2.5/5000 with toluene) drop casted on freshly cleaved mica. The quantum dots can be seen in the AFM image in Figure 4.13. In this data scan area is kept as small as possible to get a higher resolution. In AFM image of Sample-408 width is ~20nm.



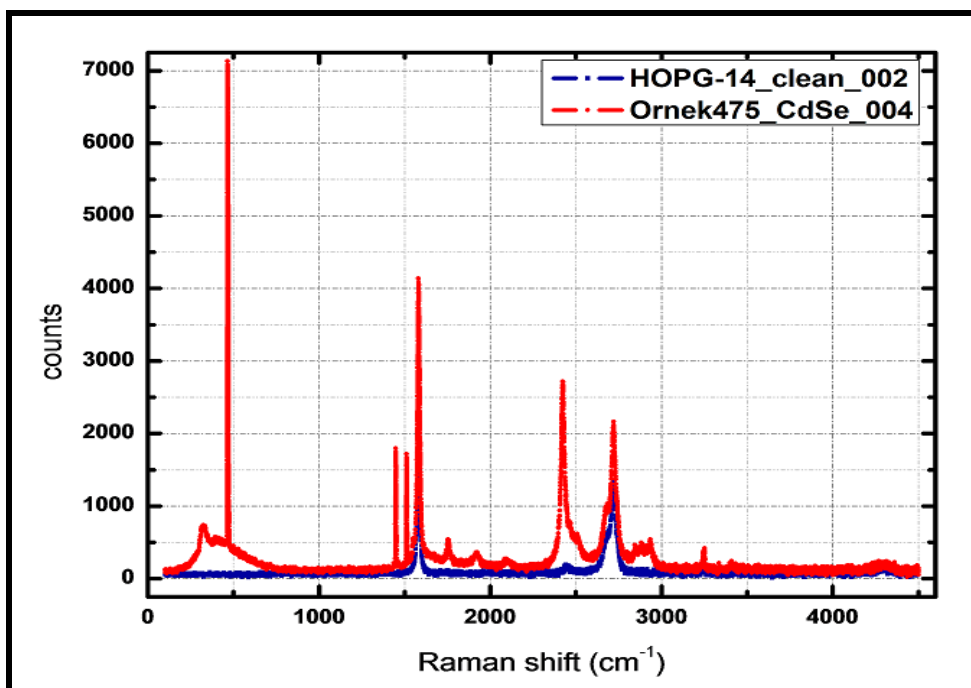
**Figure 4.13:** Sample-408, 1 μl CdSe QD Solution (Diluted by 2.5/5000 with Toluene) Drop Casted on Freshly Cleaved Mica.



**Figure 4.14:** Sample-475, 1 μl CdSe QD Solution (Diluted by 1/6000 with Toluene) Drop Casted on HOPG-9.

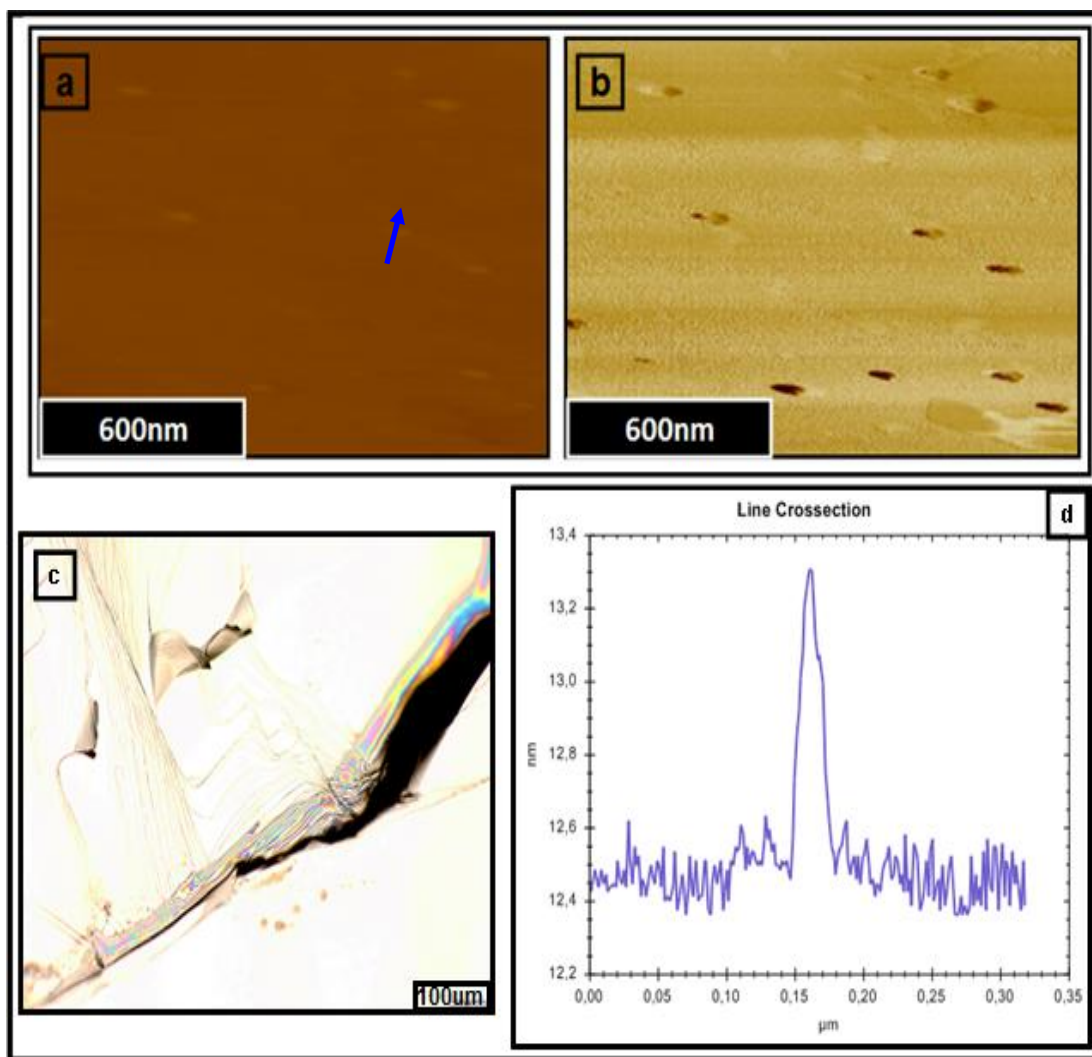
Figure 4.14 (a) shows the optical image and (b) shows the AFM image of Sample-475 and (c) is the height profile. Sample-475 was prepared and it would be scanned

with Raman spectroscopy. Before Raman it was scanned with AFM and seen that there is a thin film on the surface. This structure was observed in Sample-300 before. This film has coated whole surface. Height of this film is 3nm. HOPG steps are not observed because of this formation.



**Figure 4.15:** Raman Spectra of the Clean HOPG-14 and sample-475.

Sample 475, 1 $\mu$ lCdSe QD solution (diluted 1/6000 with toluene) drop casted on HOPG. Raman scattering spectra of CdSe QDs were measured at room temperature in the clean room using Renishaw. 532nm laser was used. Raman spectroscopy as a tool for characterization and Raman spectra provides molecular information. In Figure 4.15 several peaks are seen. Raman spectrum of bulk CdSe crystal has the value of 213  $\text{cm}^{-1}$ . The Raman peak around 210 $\text{cm}^{-1}$  for CdSe QDs. The substrate is HOPG and its peaks are around 1584 $\text{cm}^{-1}$ , 2710 $\text{cm}^{-1}$  and 3248 $\text{cm}^{-1}$ [74]. The strong sharp peak for is cosmic background. Toluene peak around 2864  $\text{cm}^{-1}$  and our peak is 2855.81 $\text{cm}^{-1}$ . It means that the carbon, quantum dot and toluene coexist.



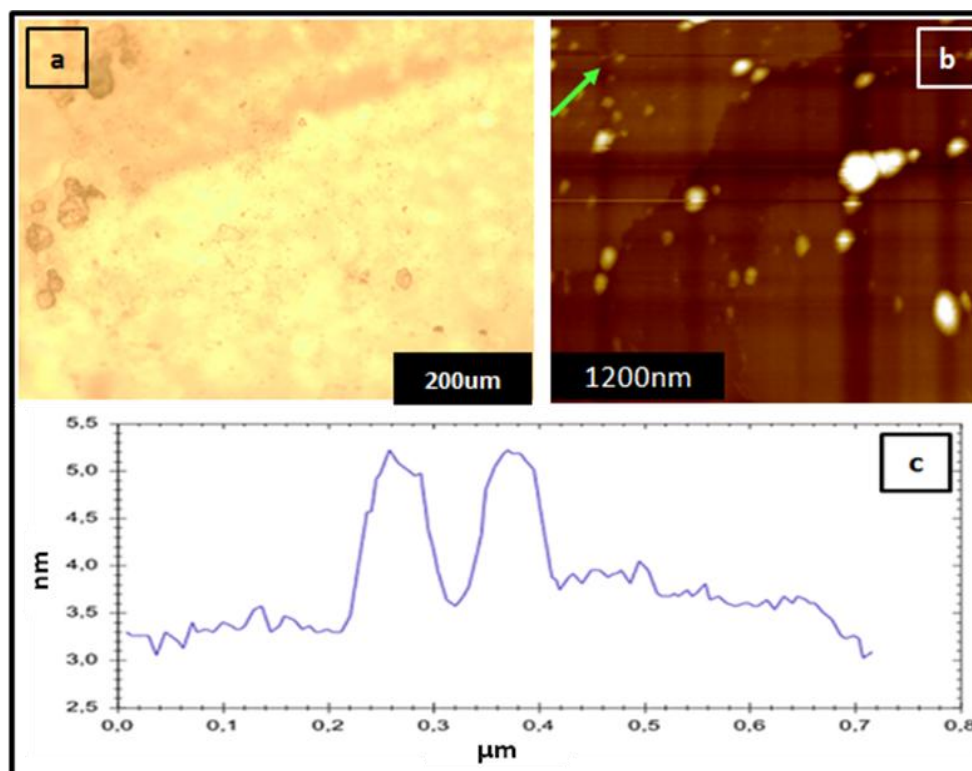
**Figure 4.16:** Sample-484, 1μl CdSe QD Solution (Diluted by 1/6000 with Toluene) Drop Casted on HOPG-9.

Sample 484 was prepared with CdSe quantum dot. 1μl QD solution (diluted by 1/6000 with toluene) was drop casted on HOPG-9. In here again diluted ratio changed. The different ratios were tried to obtain a better result. In Figure 4.16 (a) and (b) shows AFM images of Sample-484, (c) optical image and (d) height profile of Sample-484. Heights of these particles are very small, approximately ~ 1 nm, yet quantum dot particles size ~ 9-10 nm (for CdSe) then these structures are not quantum dots. It can be driven from toluene.

Until this sample CdSe core type quantum dots were used and also InP/ZnS core-shell type quantum dots will be used. Sample-423 was prepared using the another type of quantum dot. InP/ZnS particle with size ~ 5 nm (total diameter size). InP/ZnS quantum dots are in toluene and their density 1 mg/mL. 1 μL of the solution contains  $8.5 \times 10^{12}$  (see Appendix 1). Sample area is  $5 \times 5 \text{ mm}^2$ . If 1 μL QD

solution is drop casted on this area, number of quantum dots per unit area can be calculated. The numbers of quantum dots in 1 $\mu$ L quantum dot solution proportion to sample area and  $3.4 \times 10^{-1}$  QDs are obtained in 1 nm<sup>2</sup>.

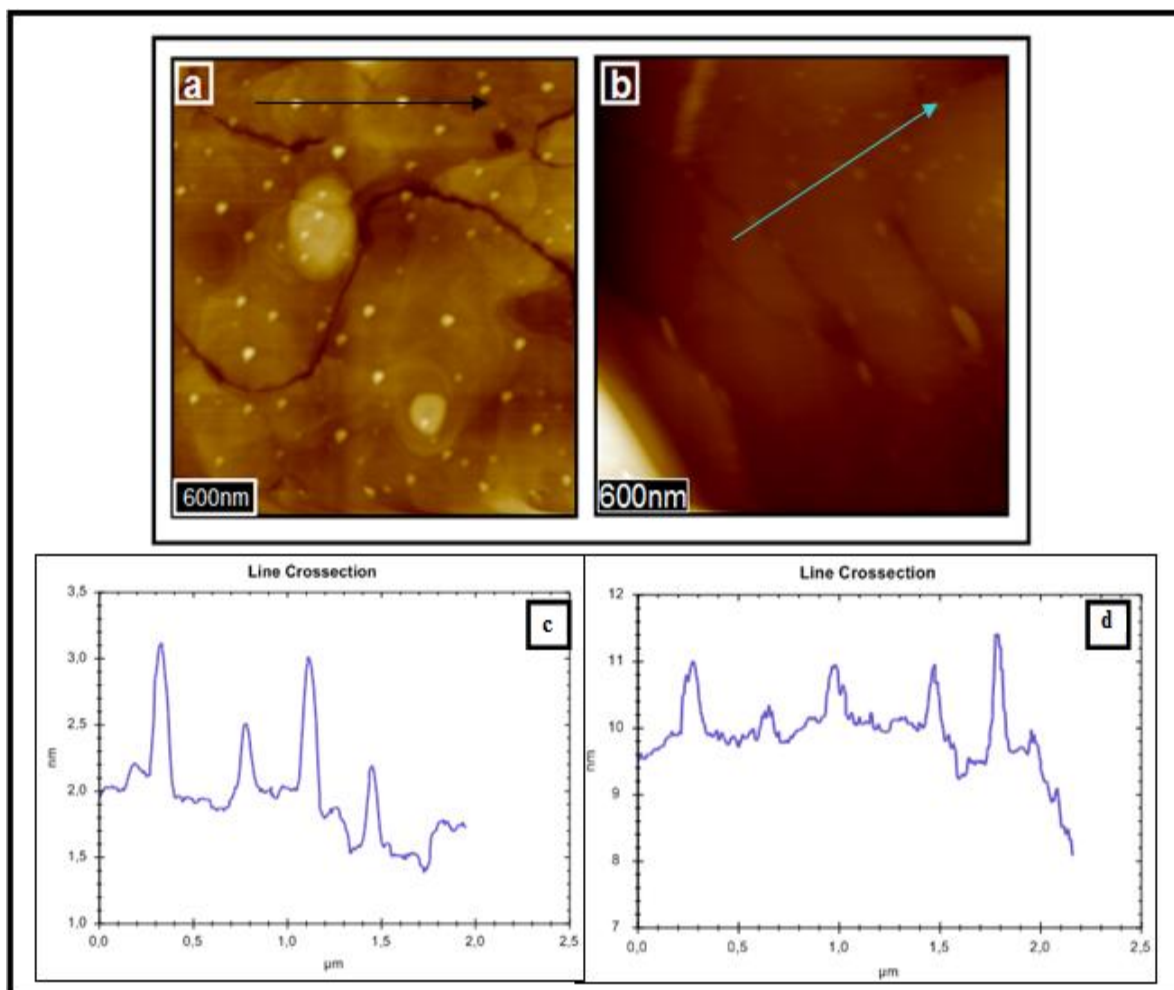
In Figure 4.17 InP/ZnS quantum dot clusters can be seen. The result is better than CdSe quantum dots. The particles are spread homogeneously and more specifically on the surfaces. The individual quantum dots may be observed by means of core-shell quantum dots.



**Figure 4.17:** Sample-423 (a) optical image, (b) topography and (c) height profile of 1 $\mu$ L InP/ZnS QD Solution (Diluted by 2.5/5000 with Toluene) Drop Casted on Freshly Cleaved Mica.

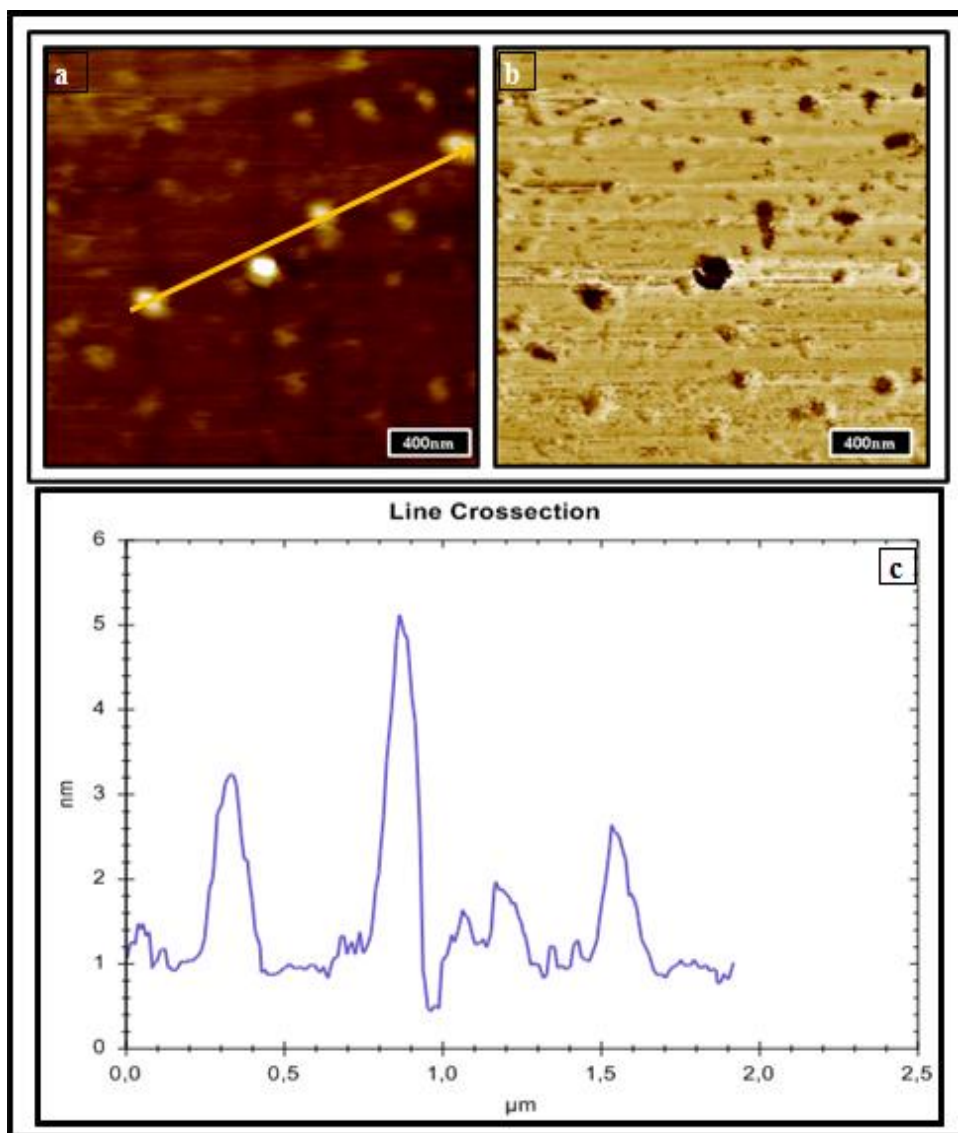
In Figure 4.18 there are two samples; before drop casted and after drop casted. Again this sample was prepared not diluted. The more dense solution on the gold surface. In (a) there are small particles but the same particles are also observed in (b). At this situation differentiating the quantum dots from the gold particles is impossible. (c) shows the height profile of the Sample-486 and (d) shows the height profile of the Sample-491. Heights of the particles are similar in both Sample-486 and Sample-491 but these heights are not similar to the size of the quantum dots.





**Figure 4.18:**(a) Sample-486, 150nm Gold Coated Mica (Au 111), (b) Sample 491,(c) and (d) are their height profiles.  $1\mu\text{l}$ InP/ZnS QD Solution Drop Casted on Sample-486 (non-diluted).

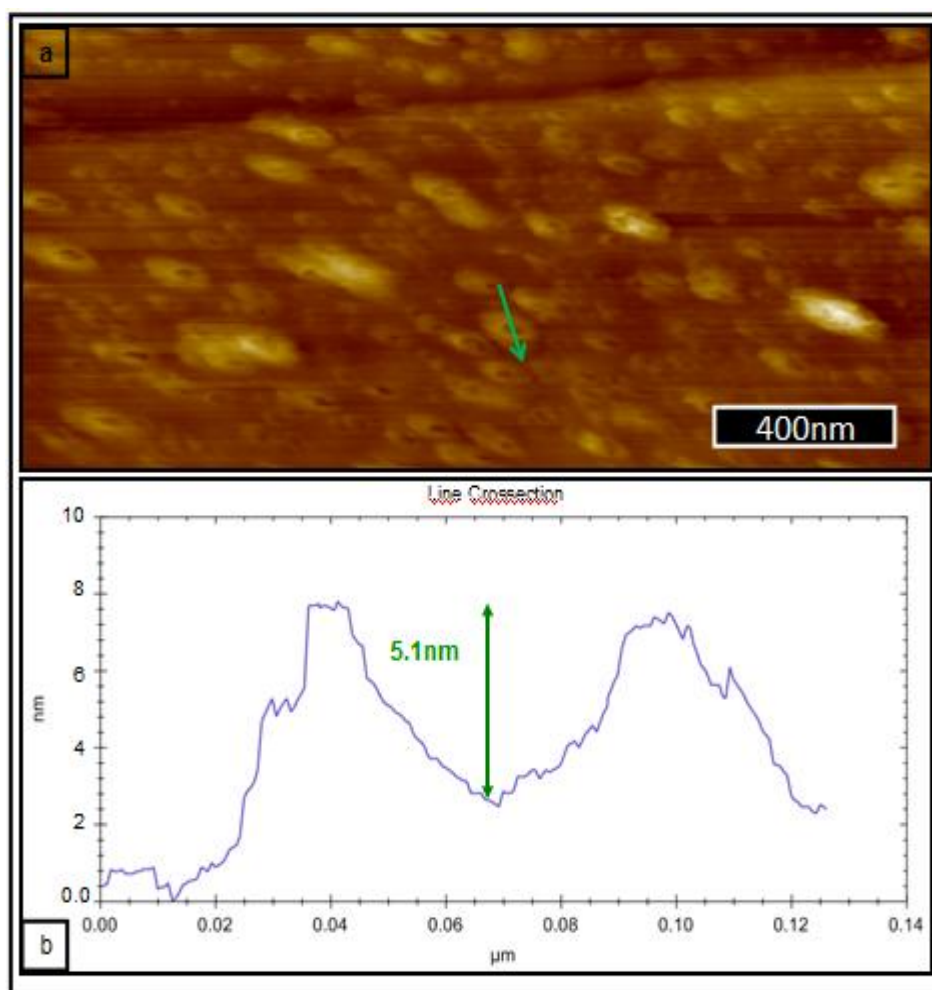
Sample-507 was prepared with InP/ZnS quantum dot.  $1\mu\text{L}$  solution was dropped on the HOPG-14. Diluted ratio is 1/6000. (Figure 4.19) Both topography image and phase image show the quantum dot cluster. Their heights are changing between 2.70nm and 4.80nm.



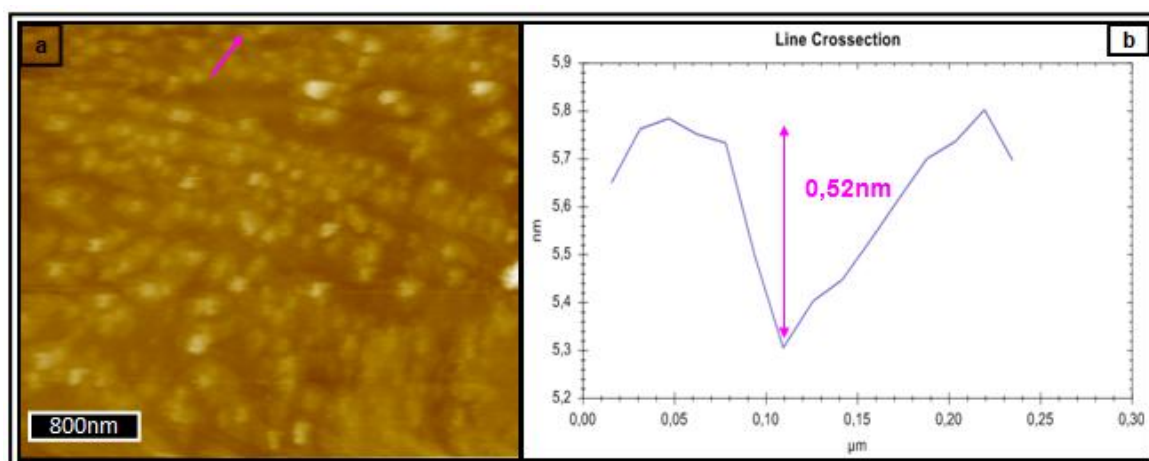
**Figure 4.19:** Sample-507, (a) topography and (b) phase and (c) height profile.

Same sample but a different area was scanned with atomic force microscope. There is a interesting result here. When the AFM image was interpreted, the dark side in the image was representing the low area. During the all quantum dot experiments, high particles on the flat surface were studied but in this data there are cavities on the surface. As if solution pierced the holes. The depths of the holes are approximately ~ 3nm,7nm and widths are changing between 20nm, 70nm.This sample will be annealed and compare with the initial state. Arrows In Figure 4.20 (b) show the holes.





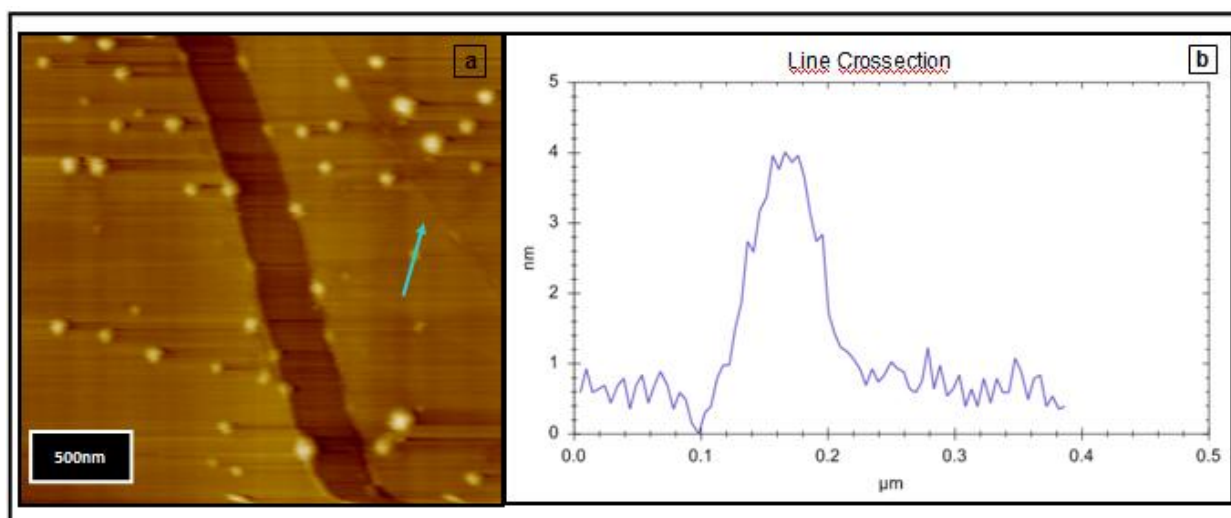
**Figure 4.20:** Sample-507, (a)topography and (b) height profile in the different area.



**Figure 4.21:** Sample-522, (a)topography and (b) height profile.

Sample-507 was annealed in tube oven in  $H_2$ -Ar atmosphere at  $100^{\circ}C$ , 1 hour. The sample which was coded as Sample-522 shown in Figure 4.21. If the Sample-507 is compared with the Sample-522, AFM images of the Sample-522 (Figure 4.21)



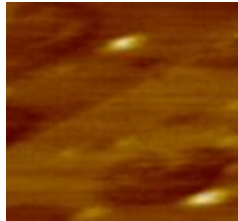
showing negligible change after annealing at 100°C. There are still holes on the surface (on the top of the particles). There is a little alteration on the height differences. The depths of the holes are approximately ~ 0,35nm, 2.5nm by comparison the initial state. AFM images showed that annealing process did not remove the contaminants which were on the surface.



**Figure 4.22:** (a) Sample-523(a) topography and (b) phase image.

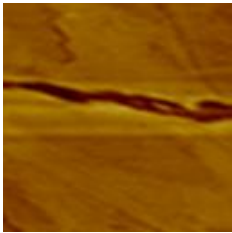

1μL InP/ZnS quantum dot solution was drop casted on the HOPG-9. The diluted ratio of this solution 1/6000 with toluene. The sample was coded as Sample-523. Quantum dots on the surface can be clearly seen. The HOPG surface is notably flat. Quantum dots spreaded. on the surface. There are a great number of quantum dots on the surface and their heights looks like different. Figure 4.22 shows the AFM images of Sample-523. Height of the film is 2.04 nm and heights of quantum dot are changing between 2nm and 5nm and their widths are between 20-30nm.

**Table 4.3 : Samples and Results-1.**

| Sample     | Substrate | Quantum Dot | QD Structure | Dilution | Data   | Result   |
|------------|-----------|-------------|--------------|----------|--|--|
| Sample-300 | HOPG      | CdSe        | core         | 1/2000   |  <p>There is a thin film on the surface.</p> | Height of the particles ~ 5.08nm and with is 70nm, so they are clusters. |
| Sample-338 | HOPG      | CdSe        | core         | 1/2000   |    | Height of the particles ~ 13nm   |
| Sample-393 | HOPG      | CdSe        | core         | 1/2000   |   | There is a thin film on the surface.                                     |

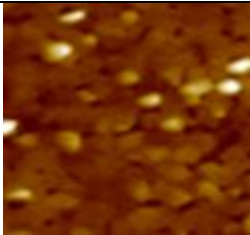
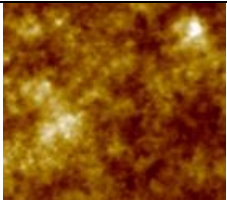
The same quantum dot and the same diluted ratio were used on the same surface. A thin film was formed. It can be driven from the toluene. On account of the fact that toluene sometimes pierce the holes on the surface or intercalates the layers.

**Table 4.4 : Samples and Results-2.**

| Sample     | Substrate | Quantum Dot | QD Structure | Dilution | Data  | Result  |
|------------|-----------|-------------|--------------|----------|---|---|
| Sample-475 | HOPG      | CdSe        | core         | 1/6000   |   | There is a thin film on the surface like Sample-300.          |
| Sample-484 | HOPG      | CdSe        | core         | 1/6000   | <br>Particle size is very small (~1nm). | These structures are not QDs, it can be derived from toluene. |


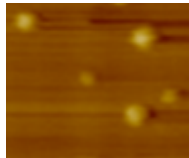
Diluted ratio was increased in order to observe smaller quantum dots but increase of dilution ratio caused the film on the surface. Toluene covered the surface.

**Table 4.5 : Samples and Results-3.**

| Sample     | Substrate | QD   | QD Structure | Dilution    | Data   | Result  |
|------------|-----------|------|--------------|-------------|--|---|
| Sample-380 | Au(111)   | CdSe | core         | 1/2000      |  | There is not certain difference between empty gold and Sample-380 |
| Sample-398 | Au(111)   | CdSe | core         | Not-diluted |  | Bright sections show the QDs clusters.                            |

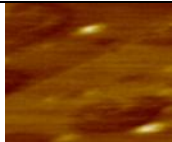
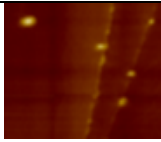

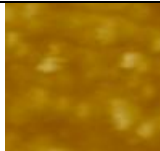
It is hard to distinguish quantum dot particles from the gold structure. Because of this, not-diluted quantum solution was used.

**Table 4.6 : Samples and results-4.**

| Sample     | Substrate | QD      | QD Structure | Dilution | Data   | Result  |
|------------|-----------|---------|--------------|----------|--|---|
| Sample-507 | HOPG      | InP/ZnS | core-shell   | 1/6000   |    | There are cavities on the top of the particles.       |
| Sample-523 | HOPG      | InP/ZnS | core-shell   | 1/6000   | <br>QD particles can be seen on the surface easily. | There is a thin film like Sample-300, Sample-475 but. |

Although Sample-507 and Sample-523 were prepared in the same conditions, their results were different. May be it was derived from the tip or the solution was not fresh.

**Table 4.7 : Samples and results-5.**

| Sample     | Subst. | QD      | QD Structure | Annealing process                           | Before  | After  |
|------------|--------|---------|--------------|---|---|--|
| Sample-411 | HOPG   | CdSe    | Core         | under $H_2 - Ar$ atmosphere, 120 °C and 1h. | <br>Contaminants disappeared after annealing.       | <br>QDs were accumulated at the HOPG steps but size of some particles increased |
| Sample-522 | HOPG   | InP/ZnS | core-shell   | under $H_2 - Ar$ atmosphere, 100 °C and 1h. | <br>There are cavities on the top of the particles. | <br>cavities on the top of the particles disappeared after annealing.           |

Annealing process became successful. When annealing process of CdSe QDs compare with InP/ZnS quantum dots, annealing for CdSe looks like very clear but some particles were connected with each others.

In this section, preparation of the quantum dot sample, dispersion of the quantum dots were discussed and the individual quantum dots were investigated. During the whole experiments different type quantum dots, surfaces, diluted ratio namely different processes were tried. Three surfaces were used; HOPG, mica and gold coated mica. HOPG and mica became more successful, gold was difficult surface in order to understand the quantum dots via AFM. Gold has a complicated granulated structure. There are small particles on the gold surface. Quantum dots particles are also small particles. It is hard to distinguish. Some stains formed on the surface such as Sample-393 and these stains were observed on the different surfaces. These stains were derived from the solvents or quantum dot solution (TOPO ligands). Toluene is very suitable as it intercalates into HOPG layers and it can be formed some structures similar to HOPG steps. After annealing these stains disappeared such as Sample-411. Annealing process is very useful method to get rid of the contaminants but it was seen that this process is more effective for CdSe quantum dots than InP/ZnS quantum dots but InP/ZnS quantum dots are more successful for quantum dot investigations than CdSe quantum dots. Because of their low-size, they can be investigated with STM whereas CdSe quantum dot particles is not available for STM. In this study, numerous samples were prepared to observe the individual quantum dots. For this, diluted ratio was changed. The quantum dot solution was diluted with toluene. Toluene can damage the surfaces or cover the surface with a thin film like Sample-300 and Sample-475. Single quantum dot could not observed. According to result InP/ZnS quantum dots look like better in order to observe the single quantum dot.

## 5. INVESTIGATION OF DNA

### 5.1 Literature Review

DNA(deoxyribonucleic acid) is a crucial biological molecule with remarkable properties for living creatures. DNA stores hereditary information.It is also important to understand its morphological structure. DNA is composed of two strands of nucleotides which are curled up in the shape of a double helix[77]. Diameter of the double stranded DNA is 2nm and length of the helical repeat is 3.4nm(distance between two nucleobases is 0,34nm). Individual DNA molecules can contain hundreds of millions of nucleotides and can be several mm long. Each nucleotide is composed of a nucleobase, a sugar residue and a phosphate group. The nucleobases; adenine (A), cytosine (C), guanine (G) or thymine (T), interact with a nucleobase in an opposing strandby hydrogen bonding; As A pairs interact with T and C pairs with G. The amount of pyrimidine (T,C) is equal to the amount of purine (A,G) according to Chargaff's rule[82]. If the amount of pyrimidine is not equals to the amount of purine, this DNA is called single stranded DNA and it consists of one strand. The phosphate groups are negatively charged and they connect the sugar residues with phosphodiester bonds between the 5'and 3'. The fabrication of DNA nanostructures begins with the self-assembly of single stranded DNA into small building block. Using these small blocks a variety of complex patterns and shapes can be created. It is known as DNA origami. When a single strand folds upon itself, motifs are formed[17]. Atomic force microscopy is the main method for studying DNA origami structures. Atomic Force Microscopy (AFM) can be used to obtain images of DNA and investigatebehavior of DNA on the surfaces. AFM can provide new knowledge about processes involving DNA.Due to their atomically flat surfaces, both HOPG and mica are used as the substrates for DNA studies. HOPG is hydrophobic and the interaction with DNA is rather weak. The presence of HOPG steps can disrupt good alignment and immobilization of DNA molecules. DNA alignment can be realized with rinsing. DNA is negatively charged because of the phosphate groups and it does not stay on the negatively charged surfaces like a mica. Mica probably the most

available surface. In order to investigate DNA molecules using AFM, samples must be immobilized onto flat and the surface modification is required to immobilize biological materials for AFM studies[77-80,82].

## 5.2 Experiments

In this study, there were five types DNA sample but only two sample were used.

### DNA sequences;

- only a
- (a-d) hybridized 4 oligos-16 hours
- (a- $\delta$ ) hybridized 8 oligos-16 hours
- (a- $\delta$ ) hybridized 8 oligos-36 hours
- (a- $\delta$ ) unhybridized and not heated 8 oligos

a: GATGCTATGCTTTGTAAGCCACGTTTCTTAGAGACCTTTCATTCTATCG

b: AGACGTACCATTTCATATTTTGGAAACATCCGTTTGGTCTCTAAG

c: ATATGGGGGGTTTAGTGTCTACCTTTAGTTACTGCTTTTGAGAGAAGG

d: TGCACCTCACTTTGCATAGCATCTTTCAATCCTGATTTTAGCAGTAACT

alpha: GGAGATACAGTTTGTGAGGTGCATTTGTGTGACTCGTTTATCAGGATG

beta: CGTGGCTTACTTTCTGTATCTCCTTTTCGATAGAATGTTTGCTCAGTCG

gamma: ATGGTTGAAGTTTTGGTACGTCTTTTCTGACTGAGCTTTCGGATGTTCC

delta: GGTAGACACTTTTCTTCAACCATTTTCCTTCTCTCATTTCGAGTCACC

In this study, 3 methods were used to prepare the DNA sample.

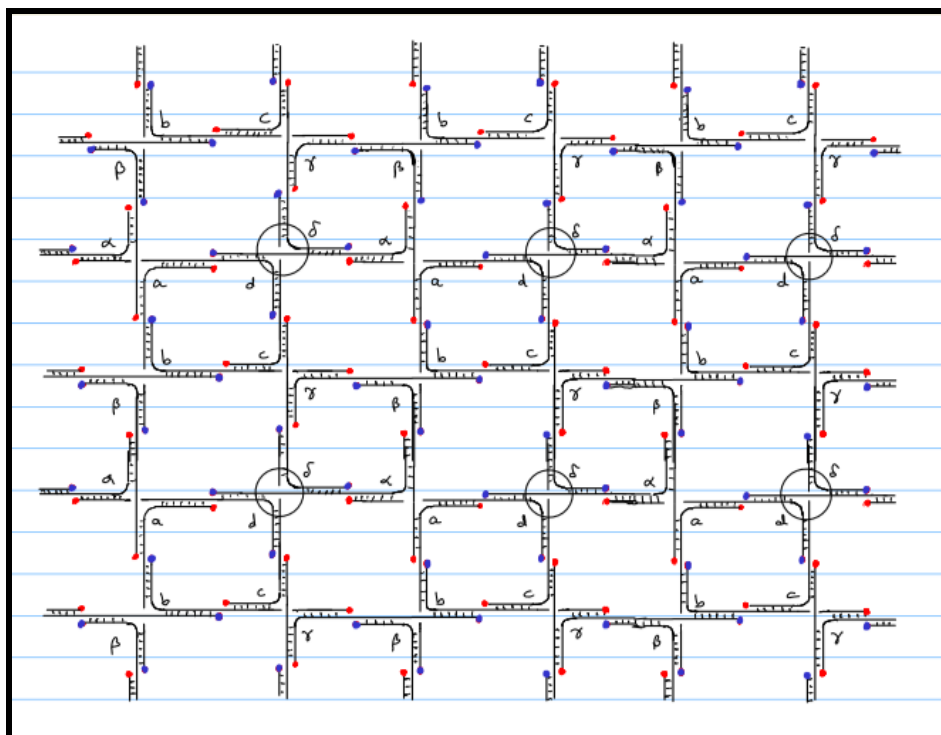
DNA solution was drop casted on the surface and placed in desiccator to dry.

DNA solution was drop casted on the surface, after a few minutes rinsed by DI water and placed in desiccator to dry.

DNA solution was drop casted on the surface. It was placed in desiccator to dry. After drying it was rinsed by DI water and again it was placed in desiccator.

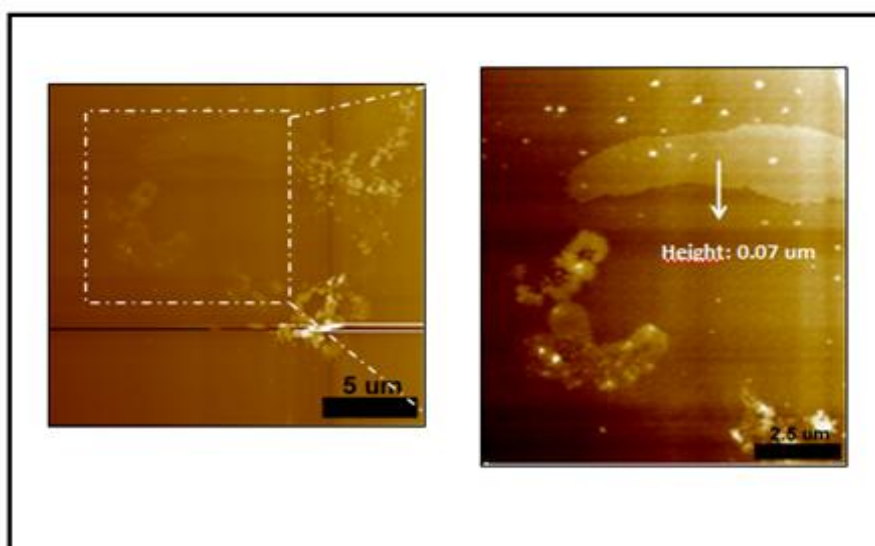
Mica and HOPG were used to prepare the DNA sample.





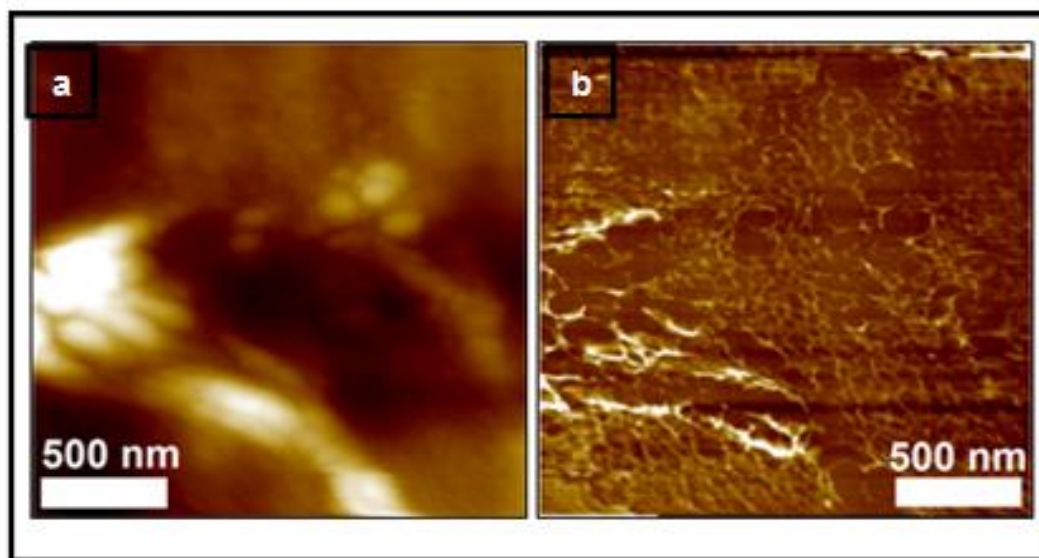
**Figure 5.1 :** Expected DNA Structure [81].

The structure in Figure 5.1 was investigated using atomic force microscope. DNA strains connect with each other and build up a structure. Lengths of each sequence is 16.32nm and their heights should be 2nm. 1 $\mu$ l solution consists 200 giga DNA molecules(see Appendix 2).

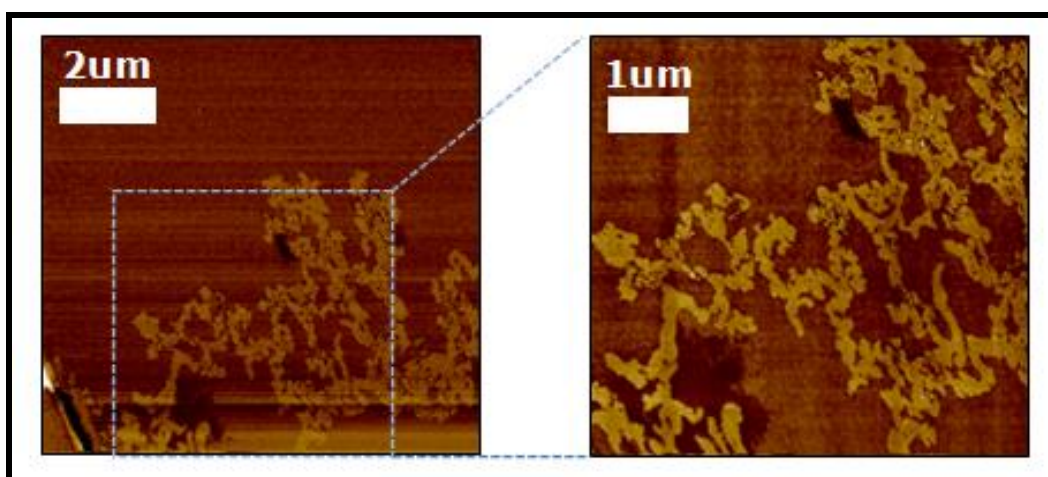


**Figure 5.2 :** 1  $\mu$ l DNA(( $\alpha$ - $\delta$ ) hybridized 8 oligos-36 hours) Solution Drop Casted on Mica Surface.

Firstly, DNA solution ((a- $\delta$ ) hybridized 8 oligos-36 hours) diluted by 1/50 with Merck water, 1 $\mu$ l DNA solution was taken with a micropipette and it was drop casted on mica. It was placed in desiccator to dry. After drying it was rinsed by DI water and again it was placed in desiccator. Network can be seen in Figure 5.2 and 5.3. The height of the network is 70nm whereas it should be 2nm. There can be a stacking at z direction.

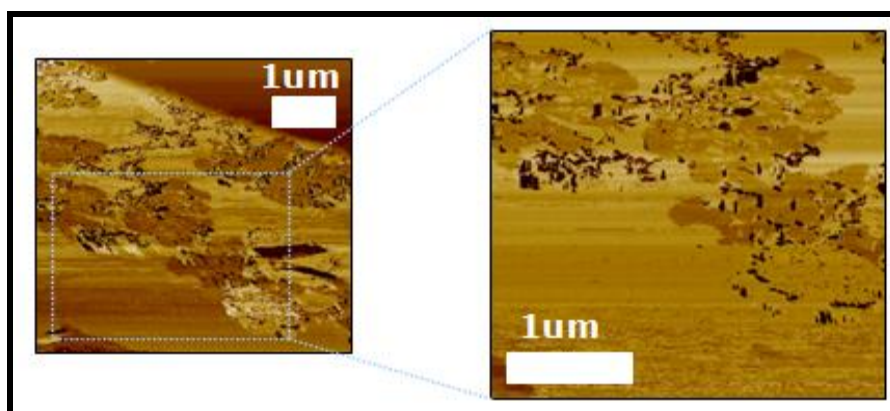


**Figure 5.3 :** AFM Images of DNA Solution Drop Casted on HOPG Surface. (a) Topography, (b) Phase Image.



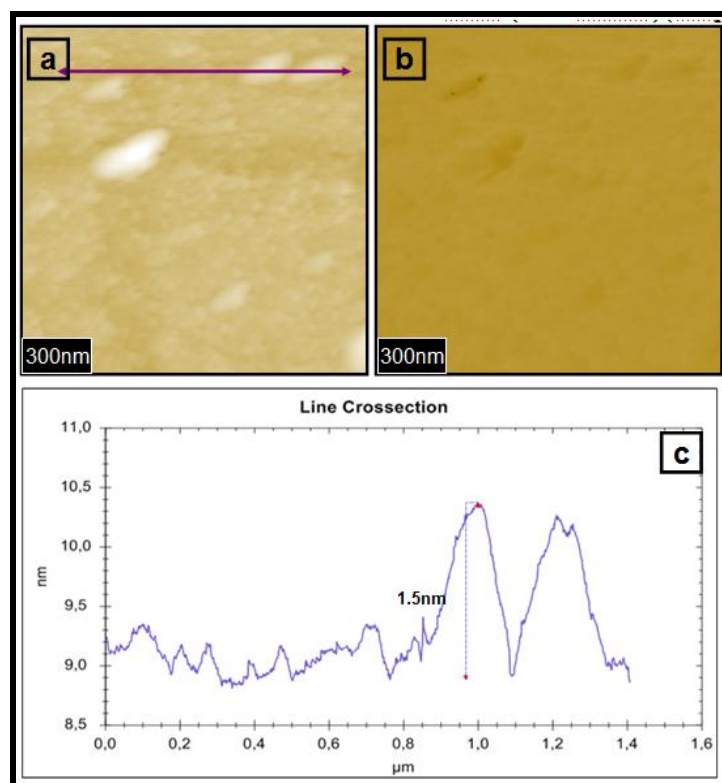
**Figure 5.4 :** Sample-351, 1 $\mu$ l DNA Solution ((a- $\delta$ ) unhybridized and Not Heated 8 Oligos) Diluted by 1/50 Drop Casted on Mica, It was Rinsed with Merck Water and Placed in Desiccator to Dry.

In here, unhybridized oligos were used and networks won't be formed. This result in Figure 5.4 is very normal. Because in this solution there are only single- stranded DNA molecules. The network structure could not design in this solution.

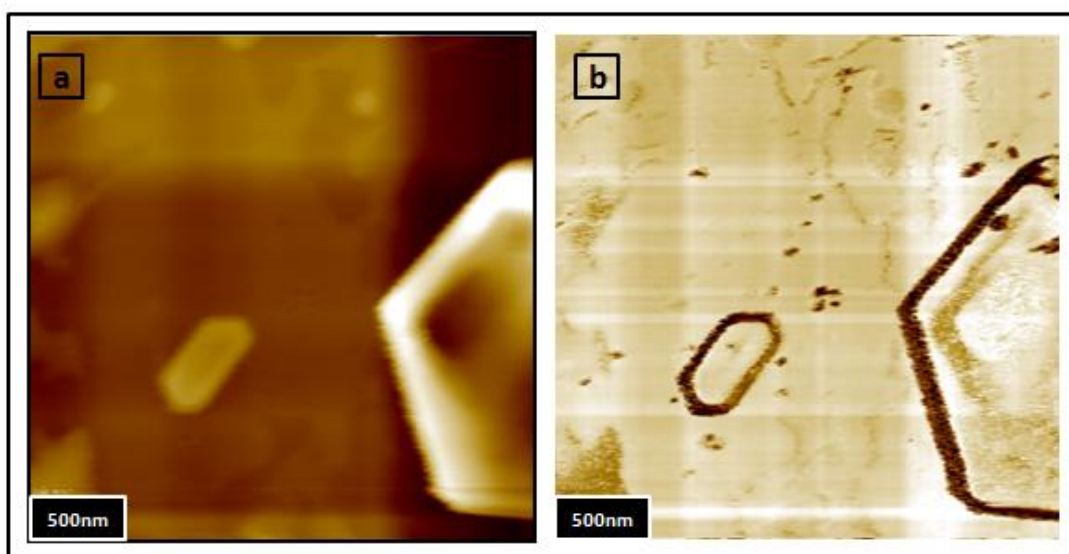


**Figure 5.5 :** Sample-350 , 1  $\mu$ l DNA Solution ((a- $\delta$ ) Unhybridized and not heated 8 oligos) diluted by 1/50 drop casted on mica, It was placed in desiccator to dry for a few minutes and rinsed with Merck Water.

Figure 5.5 show that our expectation should not be very big. Because unhybridized DNA oligos were used.

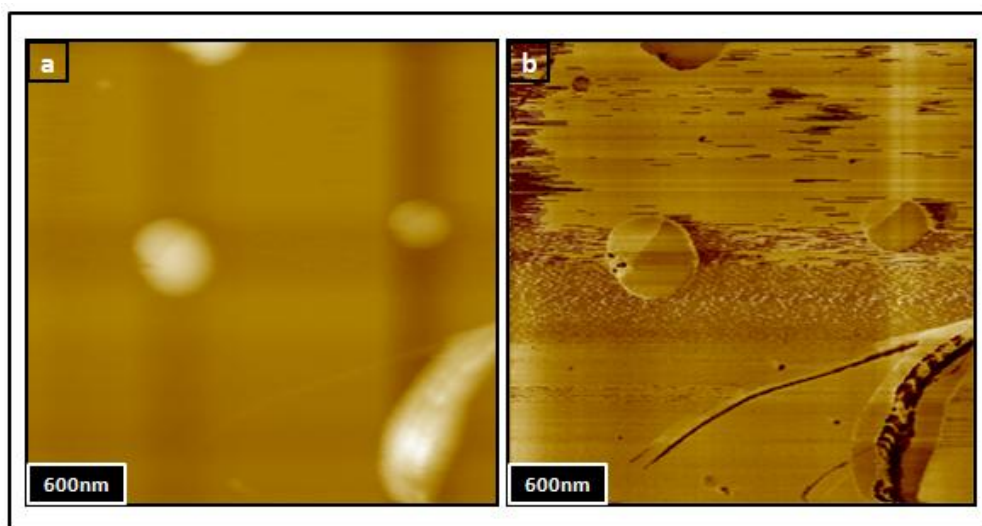


**Figure 5.6 :** Sample-490 1  $\mu$ l DNA Solution ((a- $\delta$ ) Unhybridized and not heated 8 oligos) diluted by 1/50 drop casted on mica, It was placed in desiccator to dry for a few minutes and Rinsed with Merck Water. (a)Topography, (b) Phase Image, (c) height profile.



**Figure 5.7 :** Sample-461, 1  $\mu$ l DNA Solution Drop Casted on Mica (non-Diluted).

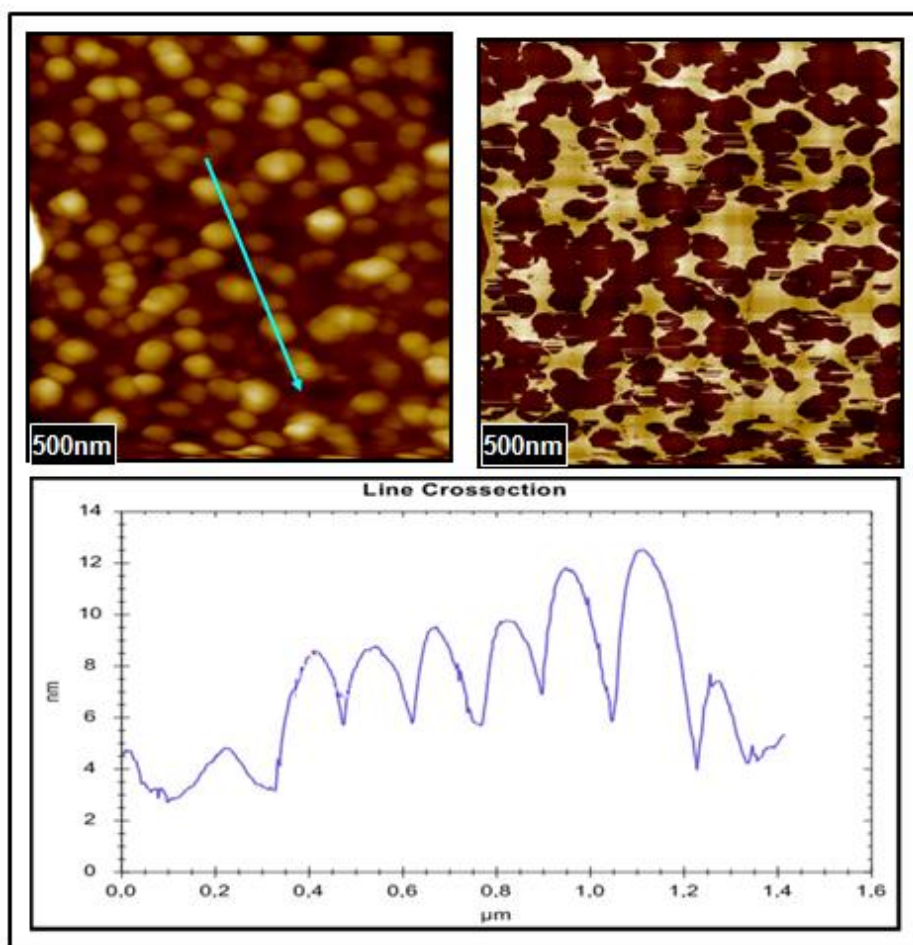
Not diluted solution drop casted on mica and hexagonal structures were observed. These structures are derived from the buffer salts. In order to remove the remnants of the salts and residues of the solution, the sample should be rinsed with doubly distilled water and dried in the air before imaging.



**Figure 5.8 :** Sample-462, 1  $\mu$ l DNA Solution Drop Casted on Mica (Diluted by 1/50)

After diluted the solution hexagonal structures were disappeared but there are balls in Figure 5.8. Sizes of the balls are between 15-30nm. These balls are big when they are compared with the sizes of DNA molecules. Their heights should be 2 nm.



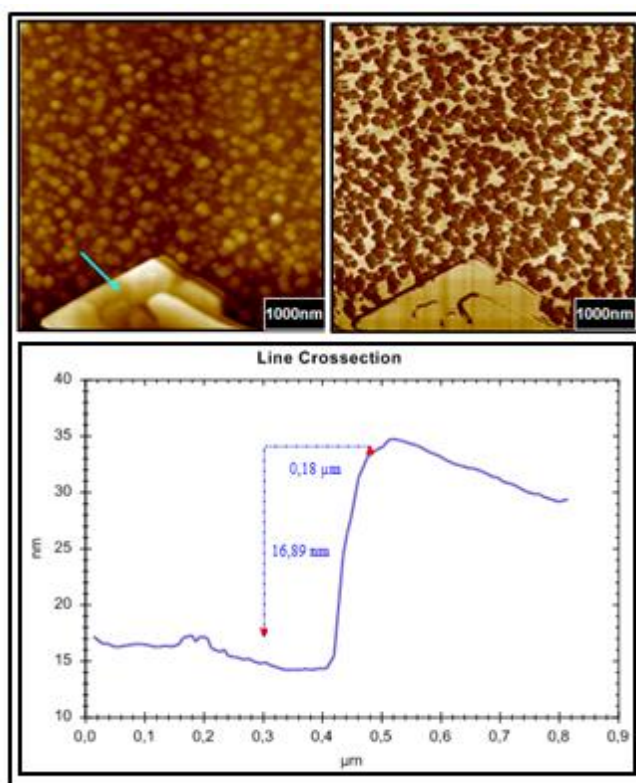


**Figure 5.9 :** Sample-501, 1  $\mu\text{L}$  DNA Solution Drop Casted on HOPG-13 (Diluted by 1/20 with Pure Water).

HOPG is a hydrophobic surface and it does not like the water but the water is remarkable solvent for the DNA solutions. It is known that water droplets stay on the HOPG surface when water drop casted on the surface using micropipette.

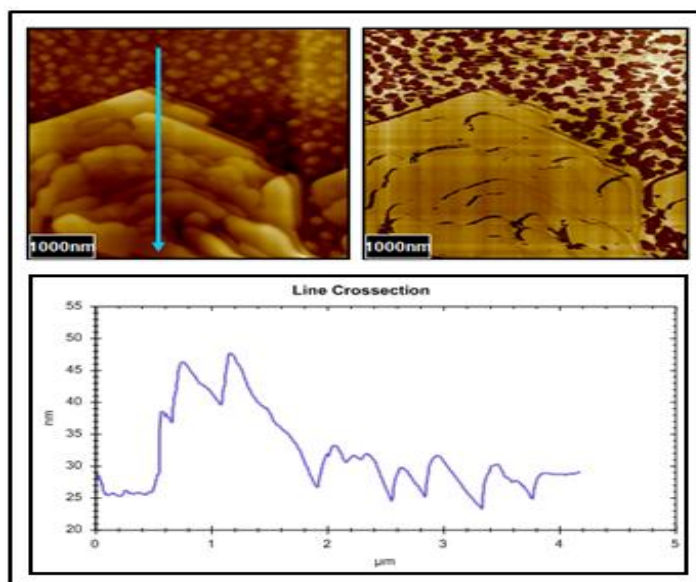
DNA solutions don't want to stay on the surface. HOPG is a difficult surface to work with DNA due to their hydrophobic surface. There are lots of balls in this data. Their size  $\sim 2.6 - 7 \text{ nm}$ .

Normally DNA solutions were diluted by 1/50 with pure water. When the directly drop casted on the surface hexagonal structures were observed. After prepare the sample, the sample was washed with pure water and hexagonal structures were disappeared. In this data DNA solution diluted by 1/20 with pure water instead of 1/50 and hexagonal structures were observed again.



**Figure 5.10 :** Sample-501, 1  $\mu\text{l}$  DNA Solution Drop Casted on HOPG-13 (Diluted by 1/20 with Pure Water) in the Different Area.

These hexagonal structures were absent firstly. Diluted ratio is getting decrease (smaller) they suddenly appeared.



**Figure 5.11 :** Sample-501, 1  $\mu\text{l}$  DNA Solution Drop Casted on HOPG-13

In Figure 5.11, hexagonal structures and DNA molecules can be seen on the HOPG surface. Height of this hexagonal- like structure is approximately 50nm.

In this section, DNA sequences procured from the KOÇ University and DNA samples were prepared with three methods. Short DNAs were used and length of each sequence was 16.32nm. There was a expected DNA structure whose shape like network. Three methods were used to prepare the DNA sample. DNA molecules were deposited on the HOPG and mica surfaces. HOPG is a hydrophobic surface and interaction with DNA is rather weak. DNA is a water soluble molecule and this causes a problem for HOPG. It is hard to distinguish the DNA structure from the water molecules on the HOPG surface. DNA is negatively charged because of the phosphate groups and it does not stay on the negatively charged surfaces like a mica. If the DNA molecules directly drop casted on the surface hexagonal structures are seen. In order to remove the remnants of the salts and residues of the solution, the sample should be rinsed with doubly distilled water and dried in the air before imaging. Hybridized and unhybridized DNA molecules were observed using atomic force microscope but their heights are changing between 15-50nm. It is very big for these structures so it can be stacking. During the DNA experiment, purchased water was used. After these experiments the results showed that purchased water is not pure and they were not appropriate water for our experiments. In order to observe the DNA structures successfully the new techniques should be discovered and tried.





## 6. CONCLUSIONS

In this study;

CdSe, InP/ZnS Quantum dots clusters were observed on HOPG, Mica and Au(111) with Atomic Force Microscope. Different QD solutions were prepared using several dilution rate to find single quantum dot and later to make electroluminescence. Quantum dots were dispersed on the surface in order to prepare the sample for P-STM. Their size should be available (small) for STM. Some contaminants, stains and thin films were observed. Stains were derived from either TOPO ligand according to literature or toluene. Toluene can intercalate the layers and this can form a structure like steps. Annealing process was used to get rid of stains and contaminations. As a results InP/ZnS core-shell quantum dots became more successful by comparison the CdSe core type quantum dots. CdSe quantum dot particle is very big and they are not observed easily by STM. Changing the diluted ratio and decreasing the scan area can be obtained the better results. Single quantum dot was not observed but smaller size quantum dot clusters were observed, particularly with InP/ZnS type quantum dots.

Effects of water and toluene on different surfaces were investigated. The water required for the DNA samples and toluene is required to prepare quantum dot solutions. Three types surface was used such as HOPG, mica, gold on mica. Mica is a hydrophilic, gold and HOPG are hydrophobic surfaces. When the water is dropped on the hydrophobic surface, the droplet stays intact on the HOPG and it affects our results badly. It is not known that these are derived from the DNA or the water. During these experiments three types DI water was used and the best water became ELGA water and it was learned that purchased water is not pure. Toluene was dropped on the HOPG to investigate the its effect on the surface. It was seen that toluene didn't create much difference on the surface. Toluene can pierce the holes or intercalate the layers.

DNA sequences procured from the KOC University and DNA samples were repaired with three methods. Behavior of the short DNAs and hybridized DNAs was searched with AFM. Mica and HOPG surfaces were used but these surfaces are not ideal for DNA. Because HOPG is a hydrophobic surface and it does not like the aqueous solutions. It is hard to distinguish the DNA structure from the water molecules on the HOPG surface. If the DNA structures are investigated on mica, both mica and DNA molecules are negatively charged. DNA molecules do not stay on the mica surface and the extra processes such as addition of ions are required in order to imaging the DNA molecules by means of AFM. During the DNA investigations some expected and unexpected structures were observed. Unexpected structures were hexagonal structures. In order to observe the DNA structures successfully the new techniques should be discovered and tried.

## REFERENCES

- [1] **Z. A. Peng, X. Peng, J. Am.** (2001). *Chem. Soc.* 123, 183.
- [2] **A. L. Rogach, T. Franzl, T.A. Klar, J. Feldmann, N. Gaponik, V.Lesnyak, A. Shavel, A. Eychmuiller, Y.P. Rakovich, J.F. Donegan, J.** (2007). *Phys. Chem. C.* , 111, 14628.
- [3] **J. Hambrock, A. Birkner, R. A. Fischer, J.** (2001). *Matter. Chem.* 11, 3197.
- [4] **J. Jortner, C. N. R. Rao.** (2002). Nanostructured advance materials,Perspectives and directions, *Pure Appl.Chem*, 74, 1491-1506.
- [5] **Ed. Marco, L.Voronin.** (2007). Frontiers in quantum dots, New York, *Nova Science*.
- [6] **D. Loss, D.P. DiVincenzo.** (1998). *Phys. Rev. A* 57, 120.
- [7] **A. Imamoglu, et al.,** (1999). *Phys. Rev. Lett.* 83, 4204.
- [8] **W. Saenger, in: Ch.R. Cantor (Ed.), Principles of Nucleic Acid Structure,** Springer-Verlag (1984).
- [9] **N.C. Seeman.** (1998). Novel DNA constructions, *Annu. Rev. Biophys.Biomol. Struct.* 27, 225 – 248.
- [10] **C. Mao, T.H. LaBean, J.H. Reif, N.C. Seeman.** (2002). Logical computation using algorithmic self-assembly of DNA triple- crossover molecules *Nature*, 407, 493 – 496.
- [11] **M.I. Pividori, A. Merkoc,i, S. Alegret,** (2000). *Biosens. Bioelectron.* 15, 291 – 303.
- [12] **H.G. Hansma, J. Vesenska, C. Siegerist, G. Kelderman, H. Morrett, R.L. Sinsheimer, V. Elings, C. Bustamante, P.K. Hansma.** (1992). Reproducible imaging and dissection of plasmid DNA under liquid with the atomic force microscope. *Science*, 256, 1180 – 1184.
- [13] **H.G. Hansma, I. Revenko, K. Kim, D.E. Laney.** (1996). Atomic force mic. of long and short double-stranded, single-stranded and triple-stranded nucleic acids, *Nucleic Acids Res.* 24, 713– 720.

- [14] **A. Sanchez-Sevilla, J. Thimonier, M. Marilley, J. Rocca-Serra, J. Barbet.** (2002). Accuracy of AFM measurements of the contour length of DNA fragments adsorbed onto mica in air and in aqueous buffer, *Ultramicroscopy*, 92, 151 – 158.
- [15] **R. Schneider, R. Lurz, G. Luder, C. Tolksdorf, A. Travers, G. Muskhelishvili,** (2001). An architectural role of the Escherichia colichromatin protein FIS in organising DNA, *Nucleic Acids Res.* 29, 5107 – 5114.
- [16] **[http://education.mrsec.wisc.edu/background/quantum\\_dots/index.html](http://education.mrsec.wisc.edu/background/quantum_dots/index.html)**. (10.12.2012)
- [17] **E. S. Andersen,** (2010). Prediction and design of DNA and RNA structures, *Elsevier*, 27, Number 3, 1871-6784.
- [18] **R. F. Tester, S. J. J. Debon, M. D. Sommerville.** (2000). *Carbohydrate Polymers* 42, 287–299.
- [19] **G. Binning, H. Rohrer, C. Gerber, E. Weibel.** (1982). *Phys. Rev. Lett.* 49, 1.
- [20] **Jane Frommer.** (1992). *Angrw. Chem. Inr. Ed. Engl.* 31, 1298-1328.
- [21] **G. Binnig, H. Rohrer,** (1987). *Reviews of Modern Physics*, part 159, 3.
- [22] **G. Binning, C. F. Quate, Ch. Gerber,** (1986). *Phys. Rev. Lett.* 56, 9, 930-933.
- [23] **M. R. Hummon, A. J. Stoll., V. Narayanamurti, P. O. Anikeeva, M. J. Panzer, V. Wood, V. Bulovic.** (2010). *Phys. Rev. B* 1098-0121, 81, 115439(8).
- [24] **K. C. Chang, Y. W. Chiang, C. H. Yang, J. W. Liou,** (2012). *Elsevier, Tzu chi medical journal*, 1-8.
- [25] **A. Engel, Y. Lyubchenko, D. Müller.** (1999). *Elsevier Sci.* 0962, 8924.
- [26] **R. Garcia, J. Tamayo, A. S. Paulo.** (1999). *Surface interf. Analy.* 27, 312-316.
- [27] **M. Gaczynska, P. A. Osmulski.** (2008). *Curr. Opin. in Coll. & Interf. Scie.* 13, 351-367.
- [28] **S. N. Magonov, D. H. Reneker.** (1997). *Annu. Rev. Mater. Sci.* 27, 175–222.
- [29] **Y. Zhang, Y. Fang, X. Zhou, X. Dong.** (2009). *Asian Journal of Control*, 11, 2, 166-174.
- [30] **G. Y. Chen, T. Thundat, E. A. Wachter, R. J. Warmack.** (1995). *J. Appl. Phys.* 77, 8.
- [31] **Marco Tortonese.** (1997). *IEEE Engineering in medicine and biology* 0739-5175/97.

- [32] **H. G. Hansma, D. E. Laney, M. Bezanilla, R. L. Sinsheimer, P. K. Hansma.** (1995). *Biophysical Journ.* 68, 1672-1677.
- [33] **J. L. Alonso, W. H. Goldmann.** (2003). *Life Sciences* 72, 2553–2560.
- [34] **K. Oura, V.G. Lifshits, A.A. Saranin, A.V. Zotov, M. Katayama.** (2003). *Surface Sci.: An Introduct. Springer* 3540005455, 9783540005452
- [35] **P. J. James, M. Antognozzi, J. Tamayo, T. J. McMater, J. M. Newton, M. J. Miles.** (2001). *Langmuir* 17, 349-360
- [36] **J. Tamayo, R. Garcia.** (1998). *Appl. Phys. Lett.* 73, 20.
- [37] **M. Yan, G. H. Bernstein.** (2006). *Ultramicrosc.* 106, 582-586.
- [38] **M. J. D. Amato, M. S. Marcus, M. A. Erikson, R. W. Carp.** (2004). *Appl. Phys. Lett.* 85, 4738.
- [39] **J. Tamayo, R. Garcia.** (1996). *Langmuir.* 12, 4430.
- [40] **S. A. Contera, H. Iwasaki, S. Suzuki.** (2003). *Ultramicrosc.* 97, 65-72.
- [41] **E. Tevaarwerk, D. G. Keppel, P. Rugheimer, M. G. Lagally, M. A. Eriksson.** (2005). *Rev. of Scie. Instr.* 76, 053707-053711.
- [42] **X. H. Qiu, G. C. Qi, Y. L. Yang, C. Wang.** (2008). *Journal of Solid State Chem.* 181, 1670-1677.
- [43] **E. M. Satoh, F. Yamada, A. Takagi, T. Matsumoto, T. Kawai.** (2009). *Nanotech.* 20, 145102.
- [44] **P. Girard.** (2001). *Inst. of phys. publ.* 12, 485-490.
- [45] **C. C. Yang, S. Li.** (2008). *J. Phys. Chem. B.* 112, 14193-14197.
- [46] **N. Tarcea, M. Harz, P. Rösch, T. Frosch, M. Schmitt, H. Thiele, R. Hochleitner, J. Popp.** (2007). *Spectrochim. Acta Part A.* 68, 1029-1035.
- [47] **V. S. Vinogradov, G. Karczewski, I. V. Kucherenko, N. N. Melnik, P. Fernandez.** (2007). *Phys. of the solid state* 50, 1, 159-162.
- [48] **M. Schmitt, J. Popp.** (2006). *J. Raman Spectrosc.* 37, 20–28.
- [49] **R. S. Das, Y. K. Agrawal.** (2011). *Vibrational Spect.* 57, 163-176.
- [50] **George J. Thomas.** (1999). *Annu. Rev. Biophys. Biomol. Struct.* 28, 1–27.
- [51] **Q. Tu, C. Chang.** (2012). *Nanomedicine: Nanotechnology, Biology, and Medic.* 8, 545–558.
- [52] **S. Berweger, J. M. Atkin, R. L. Olmon, M. B. Raschke.** (2012). *The journal of phys. chem. Lett.* 3, 945-952.

- [53] **T. Deschaines, J. Hodkiewicz, P. Henson.** (2009). Thermo Fisher Scientific Inc. 51735.
- [54] **G. Gouadec, P. Colomban.** (2007). *Progress in Crystal Growth and Characterization of Materials.* 53, 1-56.
- [55] **G. D. Smith, R. J. H. Clark.** (2004). *Journ. of Arch. Scien.* 31, 1137-1160.
- [56] **A. M. O. Brett, A. M. C. Paquim.** (2005). *Bioelectrochem.* 66, 117-124.
- [57] <http://www.2spi.com/catalog/new/hopgsub.php>. (10.12.2012).
- [58] **F. Ostendorf, C. Schmitz, S. Hirth, A. Kühnle, J. J. Kolodziej, M. Reichling.** (2008). *Nanotechnology*, 19, 305705.
- [59] **D. V. Klinov, E. V. Dubrovin, I. V. Yaminsky.** (2003). *Amer. Inst. of Phys.* 7354, 452-456.
- [60] **K. L. Mittal, Ed.,** *Contact angle wettability and adhesion* (1993).
- [61] **H. Yang, S. Y. Fung, M. Pritzker, P. Chen.** (2007). *Journal pone.* 12, 1325.
- [62] **X. Peng, L. Manna, W. Yang, J. Wickham, E. Scher, A. Kadavanich, A. P. Alivisatos.** (2000). *Nature*, 404, 59-61.
- [63] **H. P. Rocksby,** (1932). *J. Soc. Glass Tech.* 16, 171.
- [64] **Y. Yang, D. Z. Shen, J. Y. Zhang, X. W. Fan, B. S. Li, Y. M. Lu, Y. C. Liu, Y. N. Liu.** (2001). *Journal of crys. Growth*, 233, 785-790.
- [65] **M. E. Pistol, C. E. Pryor.** (2011). *The journal of phys. chem.*, 115, 10931-10939.
- [66] **A. P. Alivisatos.** (1996). *Science*, 271, 933-937.
- [67] **A. I. Ekimov, Ai. L. Efros, and A. A. Onushchenko,** (1985). *Solid State Communications*, 56, 921.
- [68] **A. M. Smith, S. Nie.** (2010). *Am. Chem. Soc.* , 43, 2, 190-200.
- [69] **B. C. Cavenett, X. Tang, C. Bradford, B. Urbaszek, T. C. M. Graham, R. J. Warburton, M. Funato, K. A. Prior.** (2002). *IEEE*, 7803, 7571, 545- 550.
- [70] **P. Mushonga, M. O. Onani, A. M. Madiehe, M. Meyer.** (2011). *Journal of nanomat.* 2012, 869284.
- [71] **S. Haubold, M. Haase, A. Kornowski, H. Weller.** (2001). *Chem. Phys. chem.* 5, 331.
- [72] **M. Green.** (2002). *Current Opinion in Solid State and Materials Scien.*, 6, 355–363.
- [73] **N. Y. Gross, M. S. Harari, M. Zimin, S. Kababya, A. Schmidt, N. Tessler.**

- (2011). *Nature mat.* , 10, 974-979.
- [74] **T. V. Torchynska, J.Douda, S. S. Ostapenko, S. J. Sandoval, C. Phelan, A. Zajac, T. Zhukov, T. Sellers.** (2008). *Journ. of non-cry. Sol.* , 354, 2885-2887.
- [75] **X.Jiang, X.Lin,** (2004). *Electrochem.Comm.*, 6, 873-879.
- [76] **E.Winfee, F.Liu, L.A.Wenzler, N.C.Seeman,** (1998). *Nature*, 394, 539-544.
- [77] **H.G.Hansma, I.Revenko, K.Kim, D.E.Laney,** (1996). *Nucleic Acids Research*, 24, No.4, 713-720.
- [78] **H.Wang, X.Wang, H.Li, X.Zhang, Y.Zhang, J.Hu,** (2011). *Langmuir*, 27, 2405-2410.
- [79] **F.Rose, P.Martin, H.Fujita, H.Kawakatsu,** (2006). *Nanotechnology*, 17, 3325-3332.
- [80] **Steven B. Smith, Yujia Cui, Carlos Bustamante,** (1996). *Science*, 271.
- [81] **Assoc. Prof. Dr.Alkan Kabakçioğlu** from Physics Department, Koç University.
- [82] **D. Mitchell, R. Bridge,** (2006). *Bioch. and Biophys. Res. Comm.* , 340, 90-94.





## APPENDIX

### APPENDIX A.1

| Crystal Structure | Lattice Constant (Å) |
|-------------------|----------------------|
| CdSe              | 6.05                 |
| InP               | 5.8687               |
| ZnS               | 5.41                 |

| Chemical Elements | Atomic Mass (amu) |
|-------------------|-------------------|
| Cd                | 112.411           |
| Se                | 78.96             |
| In                | 114.818           |
| P                 | 30.973            |
| Zn                | 65.39             |
| S                 | 32.066            |

For CdSe (640nm)( $r = 3.25 \text{ nm}$ ) ;

$$V_{\text{unit cell}} = a^3 = 0.22144 \text{ nm}^3$$

$$V_{\text{CdSe}} = \frac{4}{3} \pi r^3 = 143.72 \text{ nm}^3$$

$$N_{\text{unit cell}} = V_{\text{CdSe}} / V_{\text{unit cell}} = 143.72 / 0.22144 = 649.0245665 = \sim 649 \text{ unit cell}$$

In 1 quantum dot;

$$\text{number of Cd atoms} : 649 \times 4 = 2596$$

$$\text{number of Se atoms} : 649 \times 4 = 2596$$

Total atom in a quantum dot ; 2596 Cd + 2596 Se

Weight of a quantum dot;

$$W_{\text{CdSe}} = 2596 \times 112.411 + 2596 \times 78.96 = 496799.116 \text{ akb}$$

$$1 \text{ akb} = 1 \text{ u} = 1.660538782(83) \times 10^{-24} \text{ g.}$$

$$W_{\text{CdSe}} = 8.2495424 \times 10^{-19} \text{ g.}$$

Concentration is 5mg/mL in toluene

**So, 1 $\mu$ l solution consists (6,061 x 10<sup>12</sup>) QDs.**

For InP/ZnS (r= 5nm);

$$N_{\text{unit cell(InP)}} = V_{\text{InP}} / V_{\text{unit cell}} = 115.48515$$

$$N_{\text{unit cell(ZnS)}} = V_{\text{ZnS}} / V_{\text{unit cell}} = 8.6180905.$$

In 1 quantum dot;

$$\text{number of In atoms: } 115.48515 \times 4 = 461.9406$$

$$\text{number of P atoms: } 115.48515 \times 4 = 461.9406$$

$$\text{number of Zn atoms: } 8.6180905 \times 4 = 34.472362$$

$$\text{number of S atoms: } 8.6180905 \times 4 = 34.472362$$

$$\text{Total atoms in a quantum dot; } 461.9406 \text{ In} + 461.9406 \text{ P} + 34.472362 \text{ Zn} + 34.472362 \text{ S}$$

Weight of a quantum dot;

$$W_{\text{InP/ZnS}} = 70706.645 \text{ akb}$$

$$1 \text{ akb} = 1 \text{ u} = 1.660538782(83) \times 10^{-24} \text{ g.}$$

$$W_{\text{InP/ZnS}} = 1.1741112 \times 10^{-19} \text{ g.}$$

Concentration is 1mg/mL in toluene

**So, 1 $\mu$ l solution consists (8,517 x 10<sup>12</sup>) QDs.**

## APPENDIX A.2

$$\mathbf{T : 2.094260436 \times 10^{-22}g}$$

$$\mathbf{A : 2.243874189 \times 10^{-22}g}$$

$$\mathbf{G : 2.509558986 \times 10^{-22}g}$$

$$\mathbf{C : 1.84484883 \times 10^{-22}g}$$

In total;

|          |          |                                     |
|----------|----------|-------------------------------------|
| <b>G</b> | <b>→</b> | <b>9+8+15+6+16+10+13+5=82G</b>      |
| <b>C</b> | <b>→</b> | <b>11+14+5+13+5+11+8+15=82C</b>     |
| <b>A</b> | <b>→</b> | <b>10+11+10+12+10+8+7+10=78A</b>    |
| <b>T</b> | <b>→</b> | <b>19+16+19+18+18+20+21+19=150T</b> |

|   |          |   |
|---|----------|---|
| <b>82G: 205.783836852 x 10<sup>-22</sup>g</b> | <b>}</b> | <b>846.222693054 x10<sup>-22</sup> ng</b> |
| <b>82C: 151.27760406 x 10<sup>-22</sup>g</b>  |          |   |
| <b>78A: 175.022186742 x 10<sup>-22</sup>g</b> |          |   |
| <b>150T:314.1390654 x 10<sup>-22</sup>g</b>   |          |   |

$$1 \text{ picomole} = 17\text{ng}$$

$$1 \text{ picomole/ul} = 17 \text{ ng/ul}$$

$$17 \text{ ng} / 846.222693054 \times 10^{-22}\text{ng} = 0.2 \times 10^{12}\text{g} = \mathbf{200 \text{ giga DNA}}$$

**So, 1µl solution consists 200 giga DNA molecules.**



## **CURRICULUM VITAE**



**Name Surname: Elif PEKSU**

**Place and Date of Birth: Istanbul, 22.12.1984**

**Address: MiralayHasanKazımsok. Fırat apt. No:30/12 Şehremini - İST**

**E-Mail: elifpeksu@itu.edu.tr - elifpeksu@ gmail.com**

**B.Sc.: Trakya University, Physics**